

Discovery of Potent and Selective WDR5 Proteolysis Targeting Chimeras as Potential Therapeutics for Pancreatic Cancer

Xufen Yu,[○] Dongxu Li,[○] Jithesh Kottur,[○] Huen Suk Kim, Laura E. Herring, Yao Yu, Ling Xie, Xiaoping Hu, Xian Chen, Ling Cai, Jing Liu, Aneel K. Aggarwal, Gang Greg Wang,* and Jian Jin*Cite This: <https://doi.org/10.1021/acs.jmedchem.3c01521>

Read Online

ACCESS |



Metrics & More

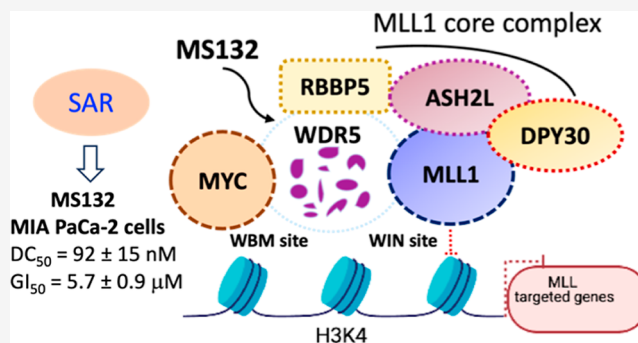


Article Recommendations



Supporting Information

ABSTRACT: As a core chromatin-regulatory scaffolding protein, WDR5 mediates numerous protein–protein interactions (PPIs) with other partner oncoproteins. However, small-molecule inhibitors that block these PPIs exert limited cell-killing effects. Here, we report structure–activity relationship studies in pancreatic ductal adenocarcinoma (PDAC) cells that led to the discovery of several WDR5 proteolysis-targeting chimer (PRO-TAC) degraders, including 11 (MS132), a highly potent and selective von Hippel–Lindau (VHL)-recruiting WDR5 degrader, which displayed positive binding cooperativity between WDR5 and VHL, effectively inhibited proliferation in PDAC cells, and was bioavailable in mice and 25, a cereblon (CRBN)-recruiting WDR5 degrader, which selectively degraded WDR5 over the CRBN neosubstrate IKZF1. Furthermore, by conducting site-directed mutagenesis studies, we determined that WDR5 K296, but not K32, was involved in the PROTAC-induced WDR5 degradation. Collectively, these studies resulted in a highly effective WDR5 degrader, which could be a potential therapeutic for pancreatic cancer and several potentially useful tool compounds.



INTRODUCTION

WD repeat domain 5 (WDR5), a highly conserved member of the WD40 repeat-containing protein family among multicellular organisms, functions as a core scaffolding component in many multiprotein complexes that are associated with epigenetic machinery and chromatin regulation.^{1–3} WDR5 has a characteristic donut-shaped seven-bladed β -propeller structure and contains two major binding sites: WDR5 interaction (WIN) site and WDR5 binding motif (WBM) site, both of which mediate the essential biological functions of WDR5.^{4–8} At the WIN site, WDR5 binds with the mixed lineage leukemia 1 (MLL1)/SET family proteins (MLL1–4, SETd1A, and SETd1B) with a set of core partner proteins, such as retinoblastoma-binding protein 5 (RBBP5), absent small homeotic-2-like protein (ASH2L), and DPY30, to form MLL1/SET core complexes that deposit histone H3 lysine 4 di- and trimethylation (H3K4me2 and H3K4me3).^{5,9} In addition, WDR5 also engages in the recruitment and localization of the oncogenic transcription factor MYC to chromatin, which promotes tumorigenesis at the opposite WBM cleft that also interacts with RBBP5.^{8,10} Aberrant WDR5 expression is associated with a wide range of cancers, including mixed-lineage leukemias,^{11–13} pancreatic,⁸ breast,^{14,15} prostate,¹⁶ gastric,¹⁷ colorectal,¹⁸ bladder cancers,¹⁹ and neuroblastoma.^{20,21} Therefore, WDR5 protein has emerged as a potential pharmacological target for treating both hemato-

logical and solid tumors. Blockage of the protein–protein interactions (PPIs) between the WDR5 WIN site and MLL1 or WBM site and MYC has been pursued to inhibit the histone methylation and suppress the transcription function of MYC, respectively.^{22,23}

Over the past decade, substantial progress has been made toward the development of WDR5 WIN-site inhibitors, including macrocyclic peptidomimetics^{24–26} and small-molecule inhibitors.^{27–35} However, most of the initial small-molecule PPI inhibitors, such as OICR-9429, showed limited effect on inhibiting cancer cell growth in vitro and in vivo models.^{28,29} In 2021, Guo's group reported a potent and orally bioavailable WDR5/MLL1 PPI inhibitor DDO-2213 that moderately suppressed the growth of MV4;11 xenograft tumors in mice.³⁶ Recently, Fesik's group and co-workers optimized their dihydroisoquinolinone-containing WDR5 WIN-site inhibitors by incorporating bicyclic heteroaryl P₇ units, resulting in potent and orally bioavailable WDR5 inhibitors that are effective in the MV4;11 xenograft tumor

Received: August 17, 2023

Revised: October 28, 2023

Accepted: November 15, 2023

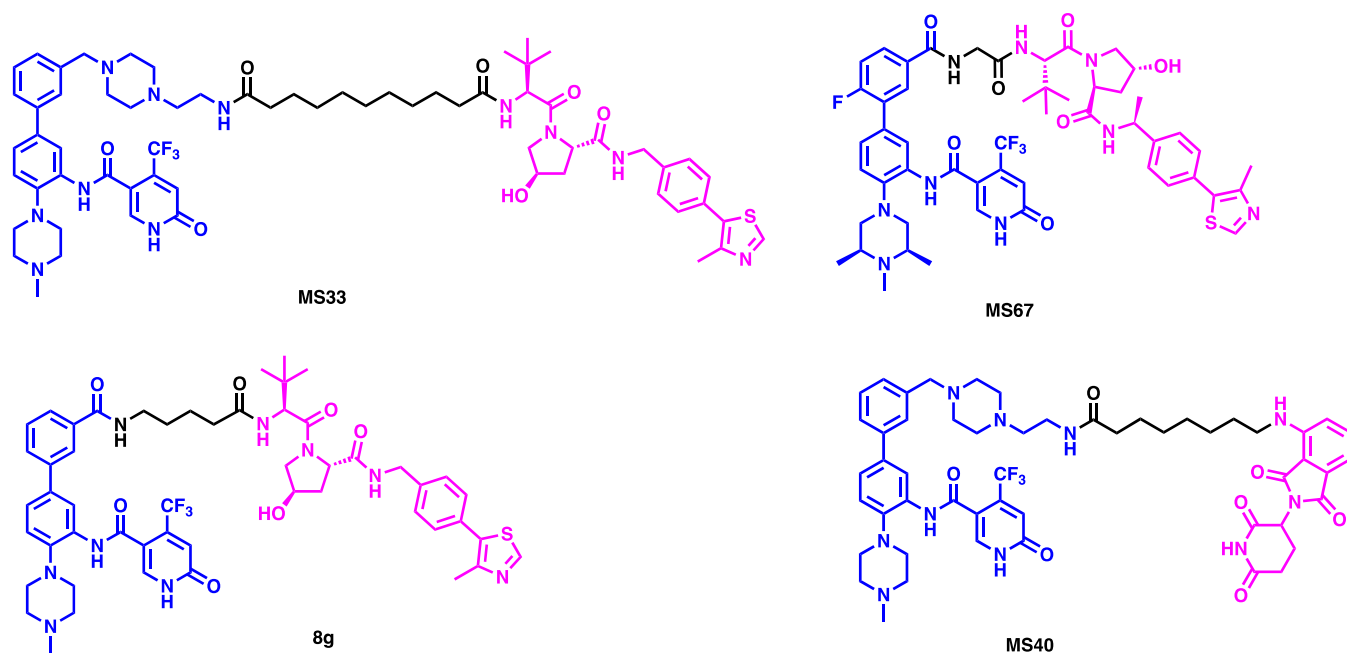


Figure 1. Chemical structures of representative WDR5 PROTAC degraders.

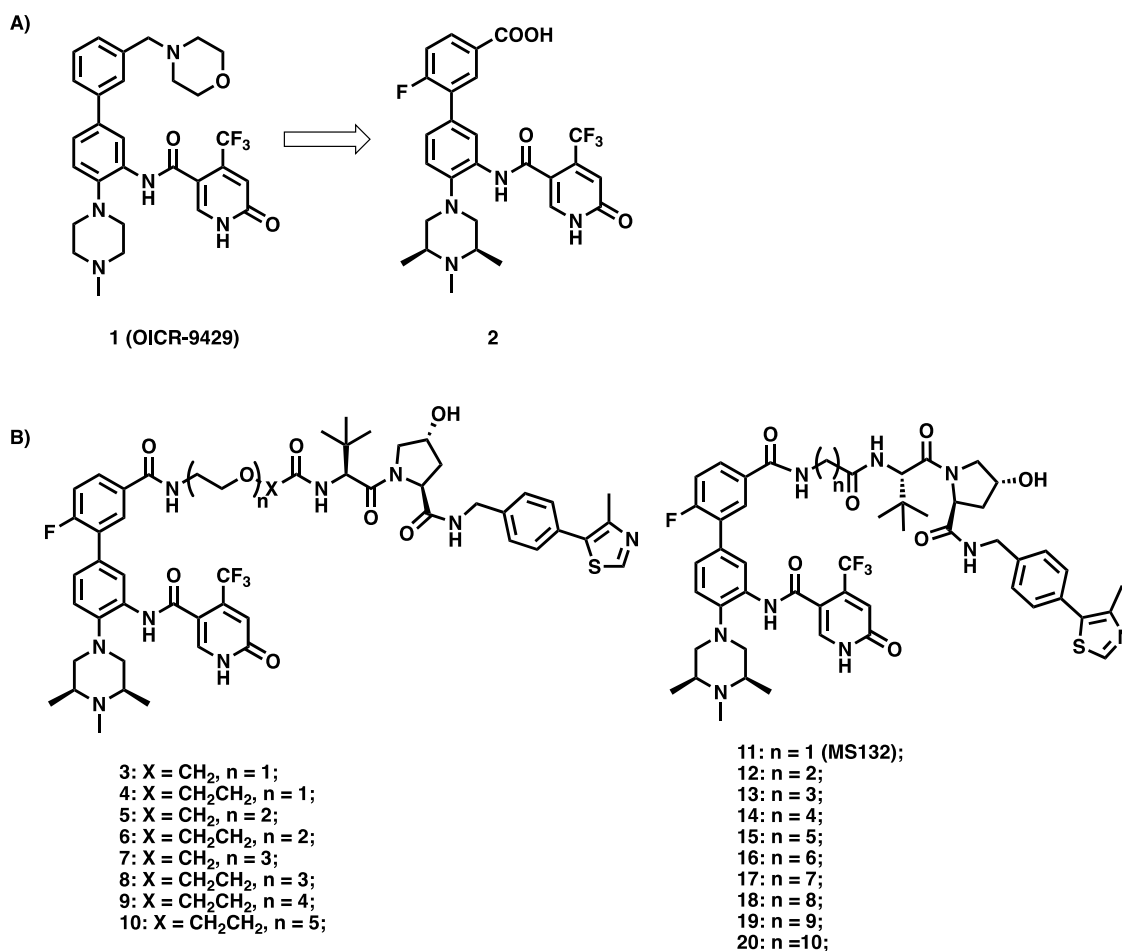


Figure 2. Schematic design of WDR5 binder precursors (A) and putative degraders (B).

models.³⁷ To date, only a few WBM site-targeting chemical probes have been discovered to disrupt the PPIs between WDR5 and MYC. However, no anticancer activity has been

reported.^{38–40} Although none of the WDR5 small-molecule inhibitors are under clinical investigation, the preclinical studies with these WDR5 PPI inhibitors have demonstrated

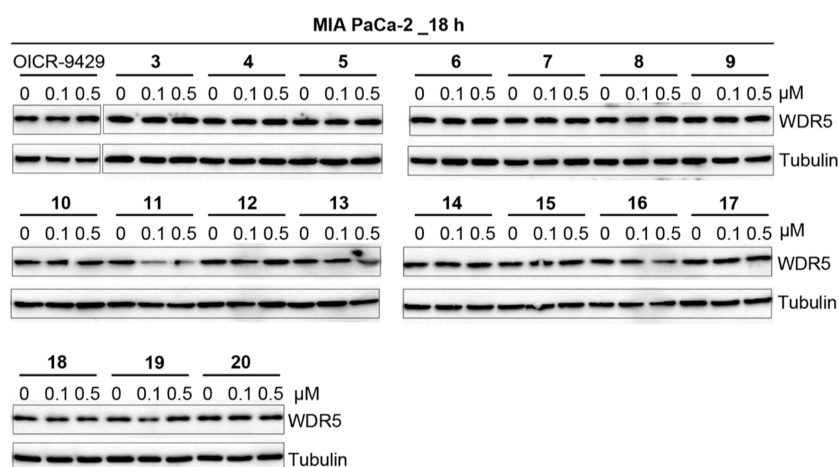


Figure 3. Effects of compounds 3–20 on inducing WDR5 degradation in MIA PaCa-2 cells. MIA PaCa-2 cells were treated with DMSO or the indicated compounds at concentrations of 0.1 and 0.5 μM , respectively, for 18 h. The cell lysates were analyzed by WB analysis to measure the WDR5 protein levels. Tubulin was used as the loading control. The results shown are representative of at least two independent experiments.

the therapeutic potential of blocking WDR5's PPIs with either MLL1 or MYC. However, because WDR5 has multifaceted scaffolding functions, these PPI inhibitors that target only one binding site are unlikely to be able to diminish all of the oncogenic functions of WDR5.

Proteolysis targeting chimeras (PROTACs) are heterobifunctional small molecules that consist of ligands to bind proteins of interest (POIs), ligands to recruit E3 ligases, and chemical linkers to connect both ligands. PROTACs bring E3 ligases into the close proximity of the POIs, leading to selective polyubiquitination and the subsequent degradation of the POIs via the 26S proteasome.^{41–45} Compared with occupancy-driven small-molecule inhibitors that specifically target the enzymatic functions of the POIs, PROTACs pharmacologically induce the degradation of the POIs, resulting in the suppression of both the enzymatic and nonenzymatic functions of the POIs.^{46,47} Recently, based on WDR5 WIN-site inhibitor OICR-9429, our group and Knapp group independently developed von Hippel–Lindau (VHL)-recruiting WDR5 PROTACs, such as MS33, MS67, and 8g (Figure 1).^{48,49} By conducting a limited structure–activity relationship (SAR) study in mixed lineage leukemia rearranged (MLL-r) leukemia cells, we discovered MS67, a potent and selective VHL-recruiting WDR5 degrader, which effectively suppressed *in vivo* tumor growth in both MLL-r cell line xenograft and patient-derived xenograft (PDX) mouse models.⁴⁸ In addition, our group also developed a cereblon (CRBN)-recruiting WDR5 PROTAC, MS40, which potently downregulated the protein levels of WDR5, IKZF1/3, and LIMD1 (Figure 1).⁵⁰ Here, we report our SAR studies in pancreatic ductal adenocarcinoma (PDAC) cells that resulted in the discovery of multiple VHL- and CRBN-recruiting WDR5 degraders, including 11 (MS132), which is a potent and selective VHL-recruiting WDR5 degrader that effectively suppressed proliferation in several PDAC cell lines and 25, which is a CRBN-recruiting WDR5 degrader that selectively degraded WDR5 over the CRBN neo-substrate IKZF1. While it has been understudied in the PROTAC field, by conducting site-directed mutagenesis studies, we also determined that WDR5 lysine 296 (K296), but not lysine 32 (K32), was involved in PROTAC-induced degradation of WDR5.

RESULTS AND DISCUSSION

Design and Biological Evaluation of VHL-Recruiting WDR5 Degraders in Pancreatic Cancer Cells. Based on our previously reported crystal structures of ternary complexes, WDR5–MS33–VCB (PDB ID: 7JTO) and WDR5–MS67–VCB (PDB ID: 7JTP), the morpholine ring in OICR-9429 (1) was not required for WDR5 degraders.⁴⁸ Therefore, a carboxylic group was anchored at the meta-position of the upper phenyl ring to bridge the WDR5 binder moiety to the linker moieties. In addition, the introduction of 2,4-dimethyl groups to the bottom methylpiperazine moiety and a fluoro group to the ortho-position of the upper phenyl ring significantly enhanced the binding affinity to WDR5 (Figure 2A).^{48,51} Based on these structural insights, we designed and synthesized a set of putative WDR5 degraders 3–20 by conjugating precursor 2 to the VHL-recruiting ligand VHL-1^{52,53} through a variety of PEG and alkyl linkers with different compositions and lengths (Figure 2B).

The WDR5 degradation effect of these putative VHL-recruiting WDR5 degraders was assessed using Western blotting (WB) analysis in a PDAC cell line, MIA PaCa-2. The cells were treated with degraders or OICR-9429 at 0.1 and 0.5 μM compound concentrations for 18 h (Figure 3). As expected, the inhibitor OICR-9429 had no effect on the protein levels of WDR5 at the tested concentrations. Compounds 3–10 bearing polyethylene glycol (PEG) linkers were unable to induce effective degradation of WDR5. On the other hand, compound 11 (MS132) with the shortest alkyl linker effectively decreased the WDR5 protein levels at both 0.1 and 0.5 μM . Compounds bearing longer alkyl linkers, 12–20, did not degrade WDR5 as effectively as compound 11. These SAR results demonstrated that a short alkyl linker is preferred for VHL-recruiting WDR5 degraders.

Design and Biological Evaluation of Novel CRBN-Recruiting WDR5 Degraders. Previously, we discovered MS40, a CRBN-recruiting WDR5 and IKZF1 dual degrader, which also had an off-target effect on inducing LIMD1 protein degradation in MV4;11 cells.⁵⁰ To improve the selectivity of CRBN-recruiting WDR5 degraders, we conducted a brief SAR study, which focused on modifying the bridge moieties that connect the linker moiety to either the E3 ligase ligand or the WDR5 ligand (Figure 4). First, we replaced the amino group

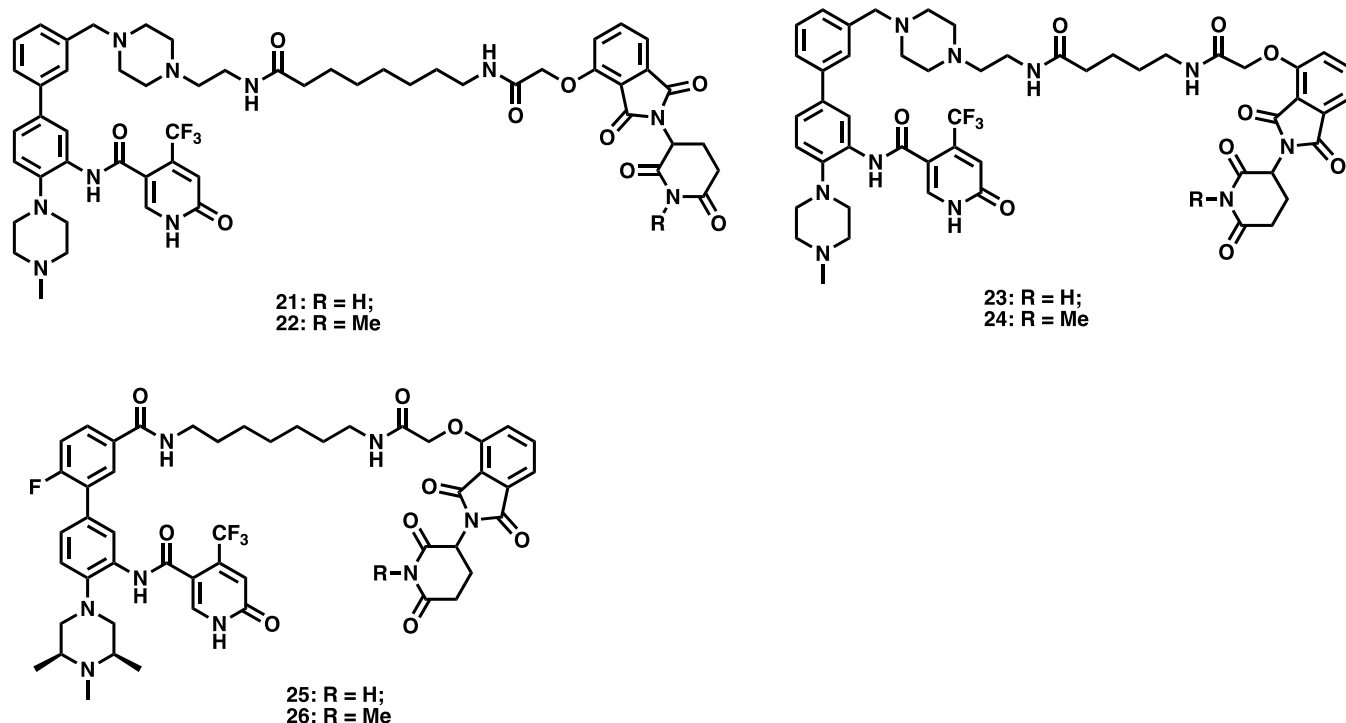


Figure 4. Chemical structures of designed CRBN-recruiting WDR5 degraders and their corresponding negative control compounds.

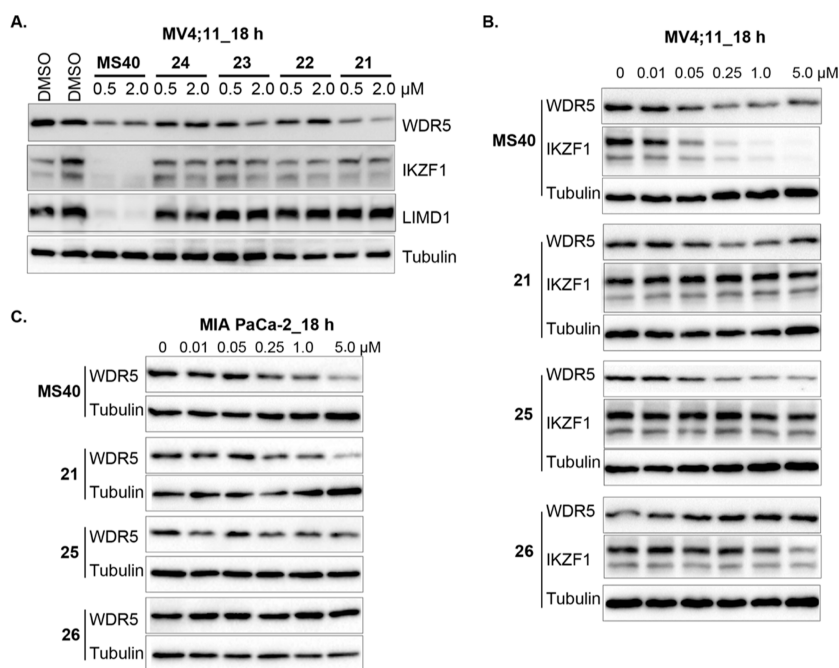


Figure 5. Effects of compounds 21–26 on reducing WDR5, IKZF1, and LIMD1 protein levels in MV4;11 and MIA PaCa-2 cells. (A) MV4;11 cells were treated with DMSO or the indicated compounds at concentrations of 0.1 and 0.5 μM , respectively, for 18 h. The cell lysates were analyzed by WB to measure the WDR5, IKZF1, and LIMD1 protein levels. Tubulin was used as the loading control. (B,C) MV4;11 (B) and MIA PaCa-2 (C) cells were treated with DMSO or the indicated compounds at the indicated concentrations for 18 h. The cell lysates were analyzed by WB to examine the WDR5 (B,C) and IKZF1 (B) protein levels. Tubulin was used as the loading control. The results shown are representative of at least two independent experiments.

of the pomalidomide moiety on MS40 with a glycolamide bridge group to provide compound 21.⁵⁴ We also designed the corresponding negative control compound 22, which contains a methylated glutarimide ring that is incapable of engaging CRBN. We next designed and synthesized another glycolamide-containing compound 23 and its corresponding

negative control 24 by maintaining the linker length of MS40. We found that 21 and 23 to a less extent effectively downregulated WDR5 protein levels, but both compounds were completely ineffective in degrading neo-substrate IKZF1, and protein LIMD1 in MV4;11 cells (Figure 5A). Notably, negative controls 22 and 24 did not have an effect on the

protein levels of WDR5, IKZF1, and LIMD1, supporting the CRBN-dependent mechanism for **21** and **23**-mediated WDR5 degradation. Moreover, as illustrated in Figure 5A, compound **21** was slightly more effective than MS40 and **23** in downregulating WDR5 protein levels. Last, we replaced the piperazinyl-containing bridge on the WRD5 binder moiety of **21** to the acetamide bridge on the intermediate **2**, to provide compound **25** (Figure 4). We also designed the corresponding negative control compound, **26**. As illustrated in Figures 5B and S1, compound **25** exhibited similar potency as **21** in degrading WDR5 protein and had no effect on IKZF1 protein levels in MV4;11 cells. As expected, the negative control **26** did not affect the protein levels of WDR5 and IKZF1. We also evaluated the effect of MS40, **21**, **25**, and **26** on degrading WDR5 in the MIA PaCa-2 pancreatic cancer cell line, which does not express IKZF1. We found that these compounds, but not the negative control compound **26**, effectively reduced the cellular WDR5 protein levels (Figure 5C). Taken together, these SAR results indicate that the α -oxyacetamide bridge added to the CRBN binder moiety significantly improved the selectivity of CRBN-recruiting WDR5 degraders, resulting in several potentially useful tool compounds such as **25** that effectively degraded WDR5 but not the CRBN neo-substrate IKZF1.

Because these CRBN-recruiting WDR5 degraders were less effective than the VHL-recruiting compound **11** in degrading WDR5 in MIA PaCa-2 cells, we selected compound **11** as a featured WDR5 degrader for further characterization in a set of biochemical and cellular assays. To study the mechanism of action (MOA) of **11**-mediated WDR5 degradation, we also designed and synthesized a structurally similar analogue of compound **11**, **27** (MS132N), by incorporating a diastereomer of VHL-1 to block the VHL engagement (Figure 6).

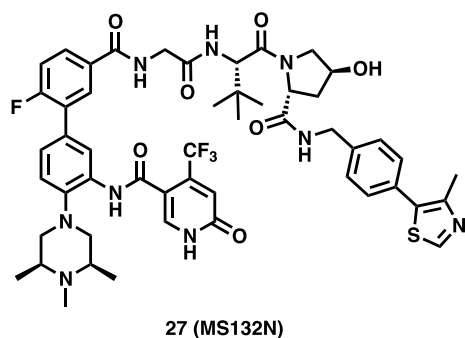


Figure 6. Chemical structure of compound **27** (MS132N), a negative control of compound **11**.

Compound 11 Induces Positive Binding Cooperativity between WDR5 and von Hippel–Lindau Elongin C–Elongin B (VCB). We first sought to determine the binding affinities of degrader **11** to the VCB E3 ligase complex and target protein WDR5 using isothermal titration calorimetry (ITC). As illustrated in Figures 7A and S2A,B, compound **11** retained high binding affinities to both VCB ($K_D = 534 \pm 48$ nM) and WDR5 ($K_D = 122 \pm 56$ nM). We next assessed binding cooperativity between WDR5 and VCB induced by compound **11** by titrating WDR5 into the saturated WDR5–**11** binary complex, with the titration of VCB into **11** as the reference. Notably, we observed a significant enhancement in VCB binding to the WDR5–**11** binary complex ($\alpha = K_D$ (binary)/ K_D (ternary) = 2.30), demonstrating that compound

11 favorably induced the formation of the WDR5–**11**–VCB ternary complex. As expected, the negative control compound **27** did not display any noticeable binding to VCB but maintained similar binding affinity to WDR5 ($K_D = 106 \pm 43$ nM) as degrader **11** (Figures 7B and S3A,B).

Compound 11 Effectively Induces WDR5 Degradation in a Concentration-, Time-, and Ubiquitin/Proteasome-Dependent Manner. We assessed the effect of compound **11** on inducing WDR5 degradation in several PDAC cell lines, including MIA PaCa-2, BxPC-3, HPAF-II, Panc10.05, and PANC-1. As shown in Figures 8A and S4, compound **11**, but not the negative control **27**, induced WDR5 degradation in a concentration-dependent manner in these PDAC cells with no “hook effect” observed at concentrations up to 50 μ M. The half maximal degradation concentration (DC_{50}) of **11**-induced WDR5 degradation was determined to be approximately 92 ± 35 nM, with the maximal level of degradation (D_{max}) of $73 \pm 12\%$ in MIA PaCa-2 cells (Figures 8B and S4). We next evaluated the kinetics of the WDR5 degradation induced by **11** in MIA PaCa-2 cells. As illustrated in Figure 8C, compound **11** effectively induced WDR5 degradation in a time-dependent manner with a significant reduction observed at 2 h and the maximal degradation achieved at 24 h. We also conducted a series of rescue experiments in MIA PaCa-2 cells to validate the MOA of **11**-mediated WDR5 degradation (Figure 8D,E). Pretreatment of MIA PaCa-2 cells with 0.4 μ M of the proteasome inhibitor carfilzomib for 2 h completely blocked **11**-induced WDR5 degradation, suggesting that the observed WDR5 degradation induced by compound **11** is mediated through the proteasome. Additionally, pretreatment with the WDR5 inhibitor OICR-9429 concentration-dependently reduced the WDR5 degradation induced by compound **11** (Figure 8E), demonstrating that WDR5 binding is required for the **11**-induced WDR5 degradation. Furthermore, the negative control compound **27** was unable to degrade WDR5 in all tested pancreatic cancer cells, indicating that the VHL E3 ligase is essential for **11**-mediated WDR5 degradation (Figure 8A, right panel). Collectively, these mechanistic studies demonstrate that the WDR5 degradation induced by **11** is mediated by the ubiquitin-proteasome system (UPS) and requires the engagement of both the target protein WDR5 and the E3 ligase VHL.

Compound 11 Is a Highly Selective WDR5 Degradation

To assess the proteome-wide degradation selectivity of compound **11**, we performed an unbiased tandem mass tagged (TMT) mass spectrometry (MS)-based global proteomic study in MIA PaCa-2 cells (Figure 9). To minimize the potential complications from secondary effects caused by WDR5 degradation, we performed proteomics analysis with a 2 h treatment rather than a longer treatment (e.g., 18 h). As shown in Figure S5, compared to DMSO treatment, compound **11** significantly reduced WDR5 protein levels after the cells were treated with **11** at 1.5 μ M for 2 h. As illustrated in Figure 9, out of 4040 quantified proteins, WDR5 is the only protein whose abundance was significantly decreased by compound **11**, with a cutoff of a P value less than 0.01 and a Log_2 fold change greater than 0.5. Overall, these quantitative global proteomic study results demonstrate that compound **11** is highly selective for inducing WDR5 degradation at an early time point (such as 2 h).

Compound 11 Effectively Suppresses the Growth of PDAC Cells. We evaluated the antiproliferative activity of compound **11** and the negative control **27** in multiple PDAC

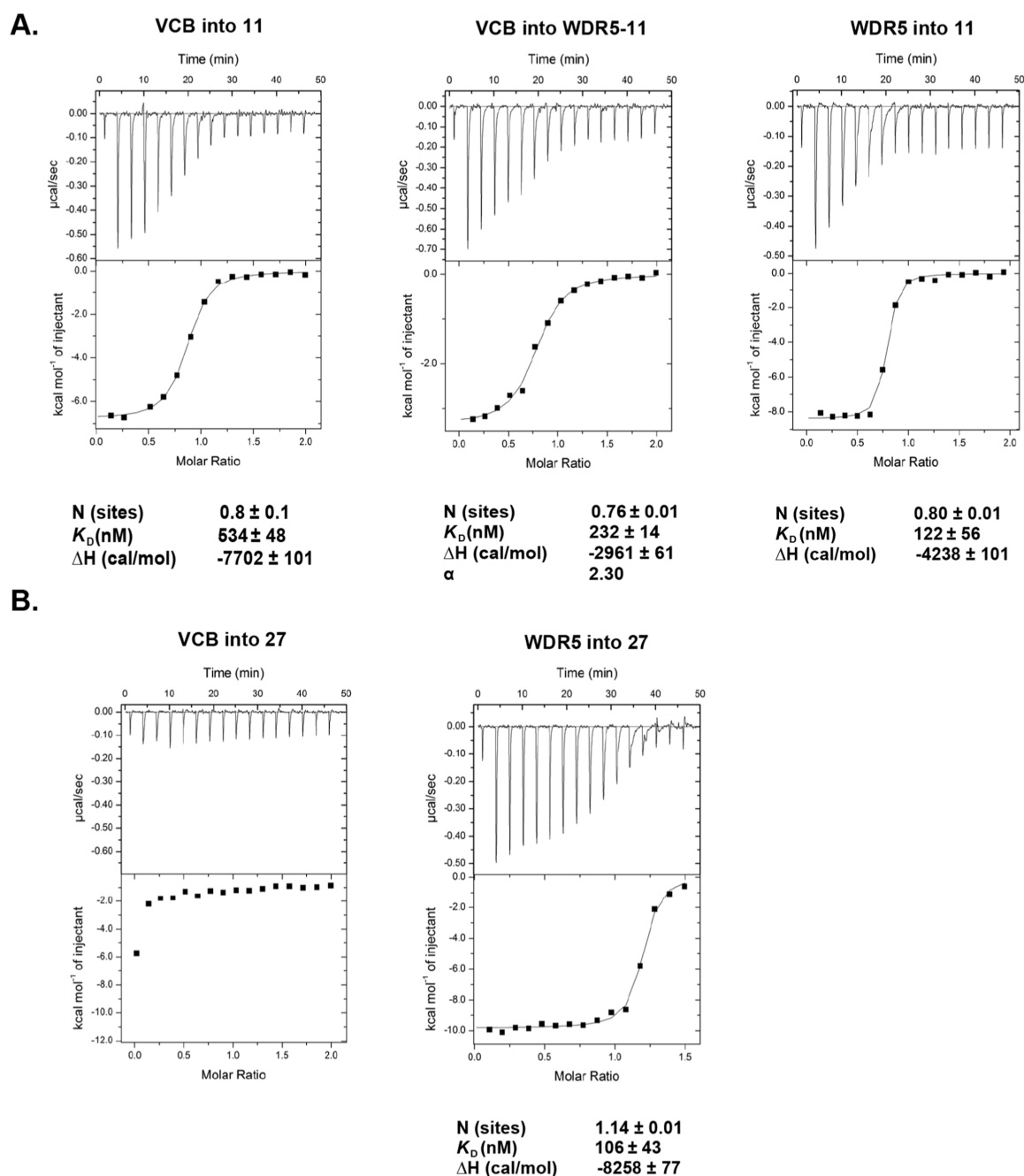


Figure 7. Compound **11** induces positive binding cooperativity between WDR5 and VCB. (A) Representative inverse ITC titrations of VCB into compound **11** (left) and **11**-WDR5 complex (middle) and of WDR5 into compound **11** (right). Three replicates of inverse ITC were performed for VCB into compound **11** (left), VCB into **11**-WDR5 complex (middle), and WDR5 into compound **11** (right) to calculate the binding kinetic and determine the cooperativity (α) for compound **11**. The calculated values represent the mean \pm SD from three independent experiments. The first injection has been removed from the fitting. (B) Inverse ITC titrations of VCB (left) and WDR5 (right) into compound **27**. Three replicates of inverse ITC titrations were performed for VCB into compound **27** (left) and WDR5 into compound **27** (right) and for measuring binding kinetics. The calculated values represent the mean \pm SD from three independent experiments. The first injection has been removed from the fitting.

cell lines including MIA PaCa-2, BxPC-3, HPAF-II, Panc10.05, and PANC-1. As shown in Figure 10A–F, compound **11**, but not the control **27**, inhibited the growth of these cells with GI₅₀ values ranging from 4.0 to 32 μ M. Of particular note, the negative control **27** did not induce any significant WDR5 degradation in all tested PDAC cell lines (Figure 8A). **27**'s lack of antiproliferative activity in PDAC cells is consistent with the lack of antiproliferative activity previously reported for the WDR5 PPI inhibitor OICR-9429.⁴⁸ Taken together, these results suggest that the WDR5 degradation induced by

compound **11** results in its antiproliferative activity in PDAC cells.

Compound 11 Is Bioavailable in Mice. We next assessed the *in vivo* mouse pharmacokinetic (PK) properties of compound **11** (Figure 11). After a single intraperitoneal (IP) injection of compound **11** at a dose of 75 mg/kg, the maximum plasma concentration ($C_{\max} = 5 \mu$ M) was achieved at 0.5 h post-treatment, and the concentrations of **11** in plasma were maintained around 1 μ M for the initial 4 h and above 100 nM over 12 h with a sufficient systemic exposure $AUC_{0\text{--}last}$

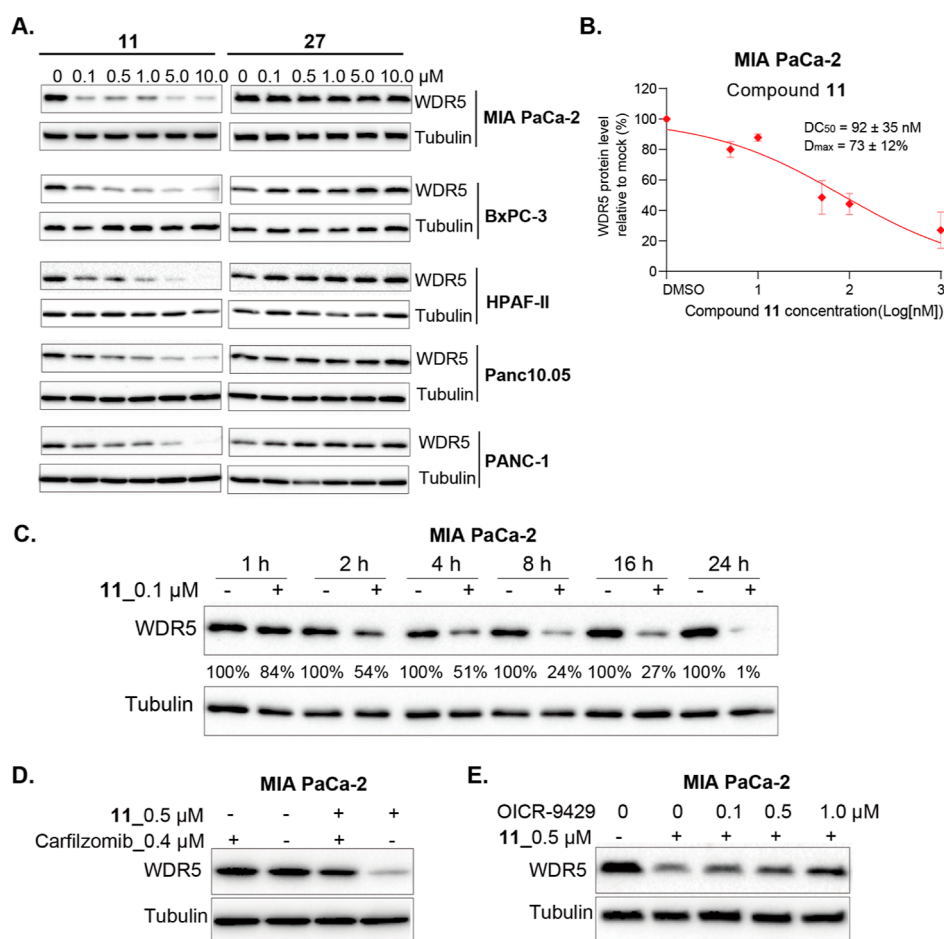


Figure 8. Compound 11 induces WDR5 degradation in a concentration-, time-, and UPS-dependent manner in PDAC cells. (A) MIA PaCa-2, BxPC-3, HPAF-II, Panc10.05, and PANC-1 cells were treated with DMSO, 11, or 27 at the indicated concentrations for 18 h. The cell lysates were analyzed by WB to examine the WDR5 protein levels. (B) WDR5 DC_{50} curve of compound 11 in MIA PaCa-2 cells, generated using the data shown in Figure S4 (from 4 independent experiments). (C) MIA PaCa-2 cells were treated with DMSO or 0.1 μ M of compound 11, and the cells were collected at the indicated time for WB. (D,E) MIA PaCa-2 cells were pretreated with 0.4 μ M of carfilzomib (D) or OICR-9429 at the indicated concentrations (E) for 2 h and then treated with DMSO or 0.5 μ M of compound 11 for an additional 4 h. Tubulin was used as the loading control in (A,C–E). The results shown in (A,C–E) are representative of at least two independent experiments.

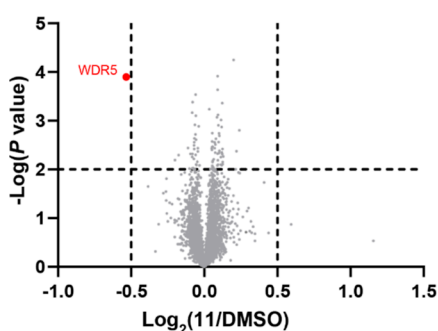


Figure 9. Compound 11 selectively induces WDR5 degradation in MIA PaCa-2 cells in an unbiased TMT MS-based global proteomic study. MIA PaCa-2 cells were treated with DMSO or 11 at 1.5 μ M for 2 h before the cell lysates were harvested for MS analysis. The dashed lines indicate a cutoff of a P value less than 0.01 (y axis) and a Log_2 fold change greater than 0.5 (x axis) in three independent biological replicates.

(area under the plasma concentration–time curve) value of 7300 h*ng/mL. These results indicate that 11 has the potential to be used in vivo animal studies. Importantly, no clinical signs were observed in the tested mice during the PK study.

WDR5 K296, but Not K32, Is Involved in PROTAC-Mediated WDR5 Degradation.

In our previously conducted structural and biophysical studies, we investigated the PPIs between WDR5 and VHL induced by our WDR5 degrader MS67 and the cross protein–ligand (MS67) interactions.⁴⁸ However, elucidation of which lysine residues of WDR5 are polyubiquitinated and are involved in PROTAC-induced WDR5 degradation has not been performed. It is worth noting that while many PROTAC degraders have been reported, very few studies have attempted to determine the lysine ubiquitination sites of the target protein in the PROTAC field. To determine which lysine residues of WDR5 are involved in PROTAC-induced WDR5 degradation, we analyzed the crystal structure of the WDR5–MS67–VCB ternary complex (PDB ID: 7JTP) we solved previously and selected K32 and K296 for examination because they are solvent-exposed residues and could be potential ubiquitination sites (Figure 12A). Next, we performed lysine-to-arginine mutagenesis to get WDR5 K32R and K296R mutants and evaluated the effect of MS67 on degrading WDR5 wild-type (WT) and K32R and K296R mutants. As expected, MS67 induced robust degradation of WDR5 WT in a concentration-dependent manner (Figure 12A). On the other hand, while the

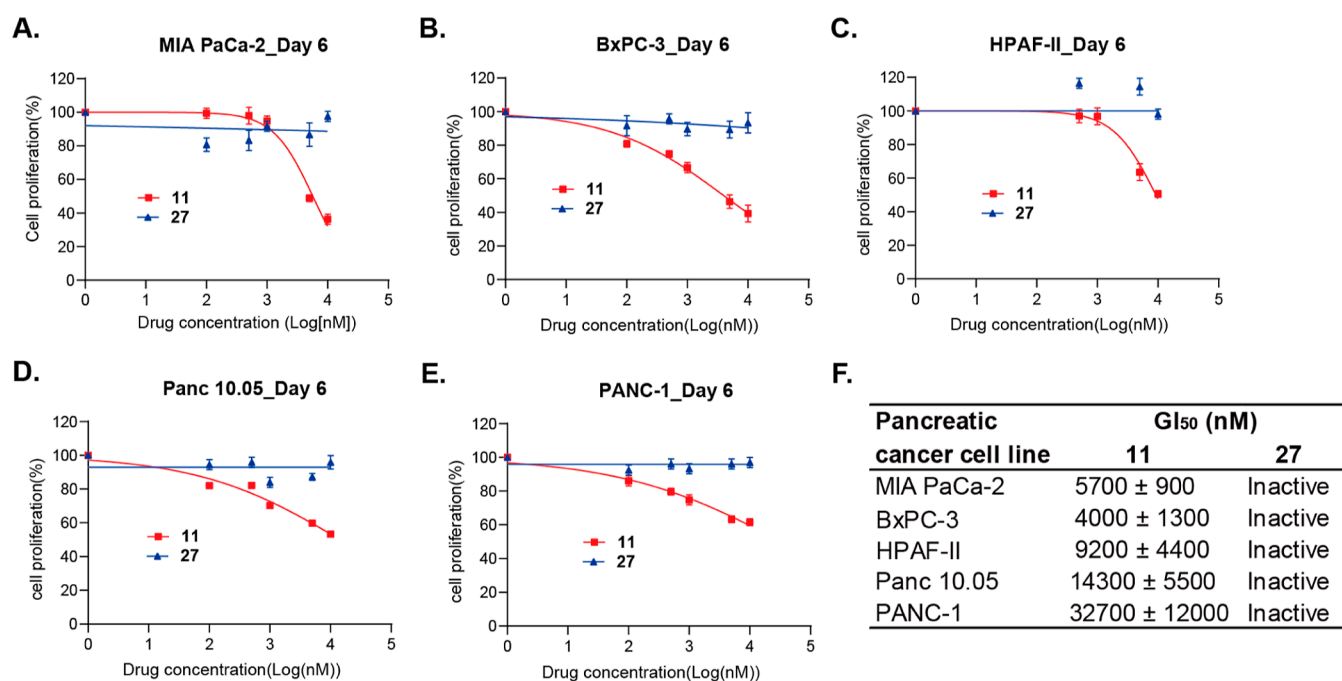


Figure 10. Compound 11 inhibits the proliferation of PDAC cells. (A–E) Growth inhibition curves of compounds 11 and 27 in pancreatic cancer cell lines, MIA PaCa-2, BxPC-3, HPAF-II, Panc10.05, and PANC-1. Y-axis, presented in the mean ± SEM of data from three independent experiments, shows the relative cell growth post-treatment with compounds 11 and 27 at the indicated concentrations (*x*-axis) for 6 days, normalized to DMSO-treated. (F) Summary of GI₅₀ values of compounds 11 and 27 in the five pancreatic cancer cell lines after a 6 day treatment.

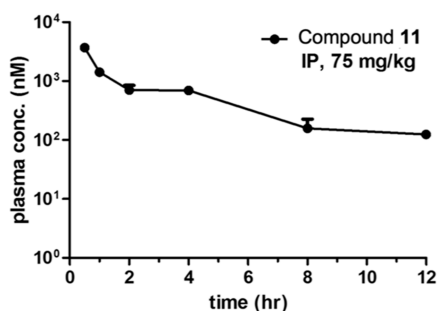


Figure 11. Plasma concentrations of compound 11 over a 12 h period in mice after a single IP injection of compound 11 at 75 mg/kg. The plasma concentrations represent the means ± SEM of data from three mice per time point.

K32R mutant displayed similar sensitivity as that of the MS67 treatment, the K296R mutant was resistant to the MS67 treatment (Figure 12B). These results suggest that K296 is likely a polyubiquitination site and is involved in PROTAC-induced WDR5 degradation.

Chemical Synthesis. The key intermediate 2 and linkers 28a–h and 29a–j were synthesized following our previously reported procedures.^{48,52,55} Compounds 3–20 were synthesized through amide-coupling of intermediate 2 and linkers 28a–h and 29a–j (Scheme 1).

The synthetic route for the preparation of compounds 21–26 is outlined in Scheme 2. Intermediate 30 and the *N*-methylated analogue 31 were prepared according to our previously reported procedures.⁵⁶ Amide coupling reactions between intermediates 30–31 and commercially available linkers 32–33, followed by *tert*-butyl ester hydrolysis, afforded carboxylic acid intermediates 34–37, which were further converted into compounds 21–24 by coupling with intermediate 38.^{48,50} Similarly, amide coupling between

intermediates 30–31 and commercially available *tert*-butyl (7-aminoheptyl)carbamate (39) and subsequent removal of the Boc-group provided intermediates 40–41. Amide coupling between 40–41 and 2 yielded compounds 25 and 26.

The synthetic route for the negative control compound 27 is outlined in Scheme 3. The diastereomer of VHL-1, 42, was prepared following our previously reported procedures.^{57,58} Amide coupling between 42 and commercially available (*tert*-butoxycarbonyl)glycine (43) and subsequent Boc-deprotection afforded intermediate 44.⁵² Amide coupling between intermediates 2 and 44 provided compound 27.

CONCLUSIONS

In summary, based on the structural insights revealed by our previously reported crystal structures of the WDR5–MS33–VCB and WDR5–MS67–VCB ternary complexes,⁴⁸ we designed and synthesized a set of WDR5 PROTAC degraders, utilizing intermediate 2 with high WDR5 binding affinity. We evaluated the effect of these compounds on degrading WDR5 in pancreatic cancer cells. From these studies, we discovered compound 11, a highly potent and selective VHL-recruiting WDR5 degrader. Compound 11 induced positive binding cooperativity between WDR5 and VCB, which led to highly effective degradation of WDR5 in five PDAC cell lines. The WDR5 degradation induced by compound 11 was dependent on the E3 ligase VHL and proteasome and occurred very rapidly (as early as 2 h). Notably, out of more than 4000 proteins detected, WDR5 is the only protein that was significantly degraded by compound 11 in an unbiased MS-based global proteomic study at an early time point (2 h). We also developed a negative control of compound 11, compound 27, which binds WDR5 but not VHL and did not degrade WDR5 in PDAC cell lines. Importantly, compound 11, but not the negative control 27, effectively suppressed the growth in

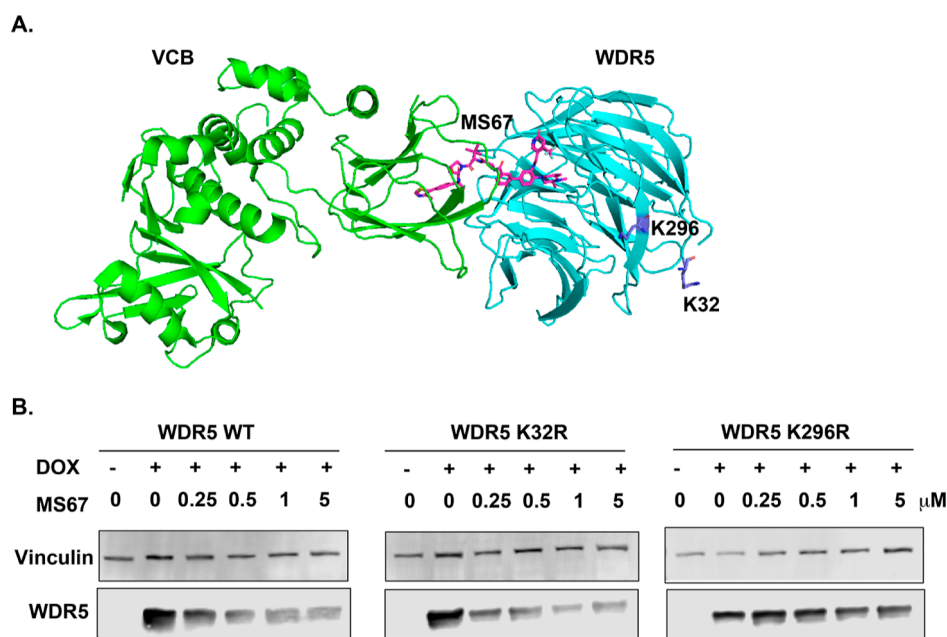
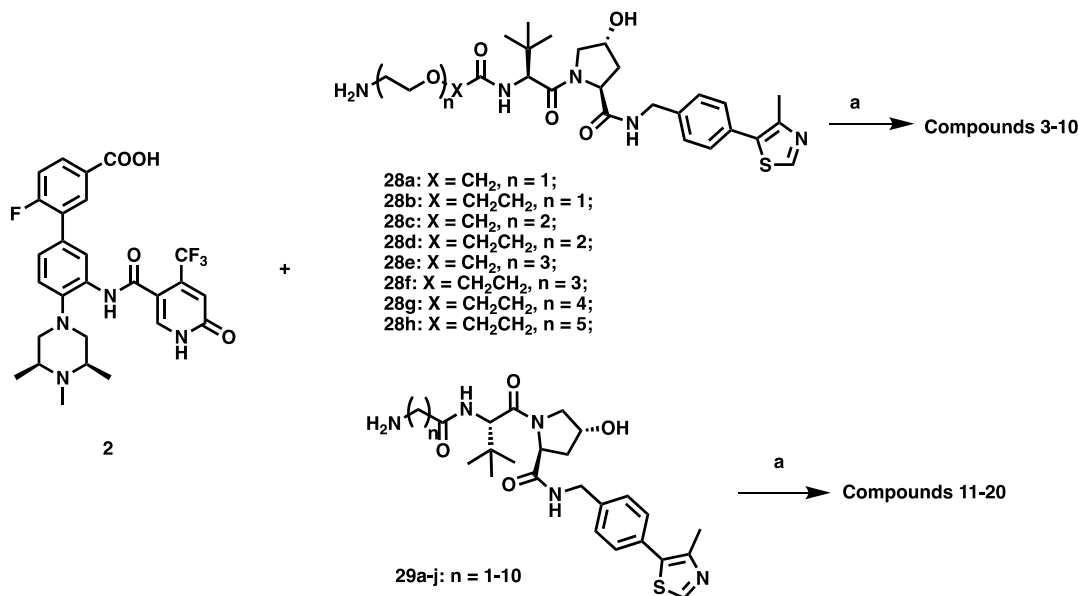


Figure 12. WDR5 K296, but not K32, is involved in PROTAC-mediated WDR5 degradation. (A) Crystal structure of the WDR5–MS67–VCB ternary complex (PDB ID: 7JTP) with WDR5 K296 and K32 residues colored in purple. (B) Immunoblot analysis of WDR5 WT (left), K32R (middle), and K296R (right) mutants after MS67 treatment. HEK293T cells, which are ectopically overexpressed with WDR5 WT, K32R, and K296R mutants, respectively, upon treatment with doxycycline (Dox), were treated with DMSO or MS67 at the indicated concentrations for 3 days. Vinculin was used as the loading control. The results shown are representative of at least two independent experiments.

Scheme 1. Syntheses of Compounds 3–20^a



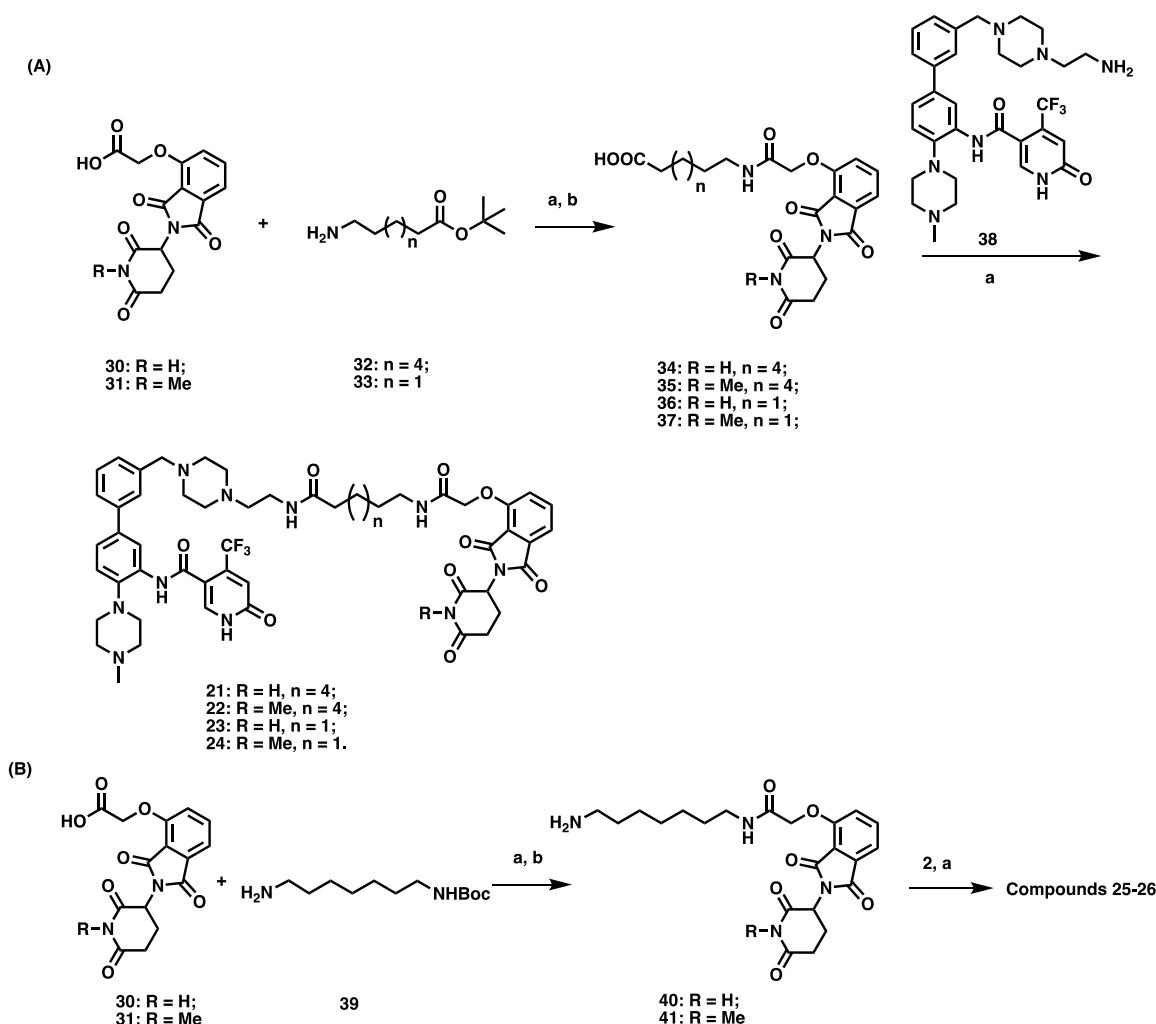
^aReagents and conditions: (a) 1-ethyl-3-(3-(dimethylamino)propyl)carbodiimide (EDCI), 1-hydroxy-7-azabenzotriazole (HOAt), N-methylmorpholine (NMM), DMSO, rt, and 12 h.

five PDAC cell lines, indicating that WDR5 degradation is the main contributor to the observed antiproliferative activity of compound **11** in PDAC cells. Moreover, compound **11** was bioavailable in a mouse PK study via IP injection, making it suitable for in vivo efficacy studies in PDAC xenograft mouse models.

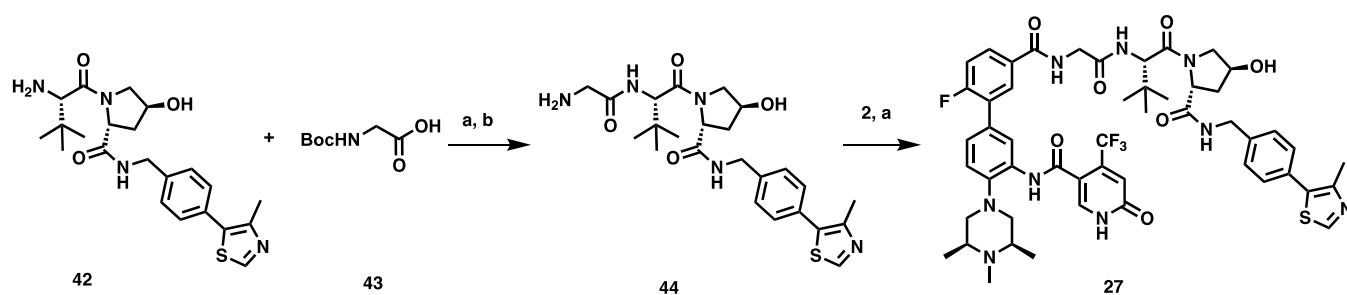
In addition, we optimized our previously reported CRBN-recruiting WDR5 degrader MS40,⁵⁰ which degraded WDR5 and the CRBN neo-substrate IKZF1. By replacing the amino group of the CRBN ligand with a glycolamide bridge, we

discovered novel and selective CRBN-recruiting WDR5 degraders, **21** and **25**, which effectively degraded WDR5 but did not degrade IKZF1.

Lastly, while a large number of PROTAC degraders have been developed for various target proteins, the studies that were intended to determine the lysine ubiquitination sites of the target protein have been scarce in the PROTAC field. To elucidate which WDR5 lysine residues are likely polyubiquitinated and are implicated in the PROTAC-induced WDR5 degradation, we conducted site-directed mutagenesis studies

Scheme 2. Syntheses of Compounds 21–26^a

^aReagents and conditions: (a) EDCI, HOAt, NMM, DMSO, rt, and 12 h and (b) TFA/DCM, rt, and 30 min.

Scheme 3. Synthesis of the Negative Control 27^a

^aReagents and conditions: (a) EDCI, HOAt, NMM, DMSO, rt, and 12 h and (b) TFA/DCM, rt, and 30 min.

and determined that WDR5 K296, but not K32, was involved in the PROTAC-induced WDR5 degradation.

Overall, we discovered a highly potent and selective VHL-recruiting WDR5 PROTAC degrader, which could be a potential therapeutic for pancreatic cancer and several selective CRBN-recruiting WDR5 PROTAC degraders, which did not degrade CRBN neosubstrates. These compounds and their corresponding negative controls are potentially useful tool compounds for further investigating the oncogenic functions of

WDR5 in pancreatic cancer and other WDR5-dependent cancers.

EXPERIMENTAL SECTION

Chemistry General Procedures. All commercially available solvents and reagents were used without further purification. Normal and reverse phase flash chromatography were performed using a Teledyne ISCO CombiFlash instrument and HP C18 RediSep Rf reverse phase silica columns, respectively. Final compounds for biological evaluation were purified with preparative high-performance liquid chromatography (HPLC) on an Agilent Prep 1200 series with

the UV detector set to 254 nm with solvent A (0.1% of TFA in water) and solvent B (acetonitrile) as eluents with a flow rate of 40 mL/min at room temperature. Purities of the final compounds were assessed at >95% by HPLC under the following conditions: Agilent 1200 series system, 2.1 mm × 150 mm Zorbax 300SB-C18 5 μm column, 1–99% gradient of 0.1% TFA in water, and 0.1% TFA in acetonitrile; flow rate, 0.4 mL/min; high-resolution mass spectra (HRMS) data were acquired on an Agilent G1969A API-TOF with an electrospray ionization (ESI) source. Proton (¹H NMR) and carbon (¹³C NMR) nuclear magnetic resonance spectra were recorded on either an AVANCE NEO 600 or 400 MHz NMR spectrometer and reported in parts per million (ppm) on the δ scale in the following format: chemical shift, multiplicity (s = singlet, d = doublet, t = triplet, q = quarter, and m = multiplet), coupling constant (J, Hz), and integration. Intermediates 2, 28a–h, 29a–j, 30–31, 38, and 42 were synthesized following our previously reported procedures.^{52,55,56}

N-(2'-Fluoro-5'-((2-(2-((S)-1-((2S,4R)-4-hydroxy-2-((4-(4-methylthiazol-5-yl)benzyl)carbamoyl)pyrrolidin-1-yl)-3,3-dimethyl-1-oxobutan-2-yl)amino)-2-oxoethoxy)ethyl)carbamoyl)-4-((3S,5R)-3,4,5-trimethylpiperazin-1-yl)-[1,1'-biphenyl]-3-yl)-6-oxo-4-(trifluoromethyl)-1,6-dihydropyridine-3-carboxamide (3). To a solution of intermediate 2 (11.9 mg, 0.022 mmol) in DMSO (1 mL) were added linker 28a (12.4 mg, 0.022 mmol, 1.0 equiv), EDCI (6.3 mg, 0.033 mmol, 1.5 equiv), HOAt (4.5 mg, 0.033 mmol, 1.5 equiv), and NMM (6.7 mg, 0.066 mmol, 3.0 equiv). After stirring overnight at room temperature, the resulting mixture was purified by preparative HPLC (10–100% methanol/0.1% TFA in H₂O) to afford compound 3 as a white solid (15.1 mg, yield 65%). ¹H NMR (600 MHz, CD₃OD): δ 8.93 (s, 1H), 8.14 (s, 1H), 8.05–7.99 (m, 2H), 7.94–7.87 (m, 1H), 7.49–7.34 (m, 6H), 7.28–7.18 (m, 1H), 6.92 (d, J = 3.2 Hz, 1H), 4.68 (s, 1H), 4.59–4.47 (m, 3H), 4.36–4.30 (m, 1H), 4.13–4.00 (m, 2H), 3.88–3.82 (m, 1H), 3.79–3.67 (m, 5H), 3.64–3.57 (m, 2H), 3.55–3.46 (m, 2H), 3.38–3.30 (m, 2H), 2.98 (d, J = 3.4 Hz, 3H), 2.44 (s, 3H), 2.24–2.18 (m, 1H), 2.10–2.05 (m, 1H), 1.47–1.39 (m, 6H), 0.97 (s, 9H). HRMS (*m/z*): for C₅₃H₆₂F₄N₉O₈S⁺ [M + H]⁺ calcd, 1060.4373; found, 1060.4389.

N-(2'-Fluoro-5'-((2-(3-((S)-1-((2S,4R)-4-hydroxy-2-((4-(4-methylthiazol-5-yl)benzyl)carbamoyl)pyrrolidin-1-yl)-3,3-dimethyl-1-oxobutan-2-yl)amino)-3-oxopropoxy)ethyl)carbamoyl)-4-((3S,5R)-3,4,5-trimethylpiperazin-1-yl)-[1,1'-biphenyl]-3-yl)-6-oxo-4-(trifluoromethyl)-1,6-dihydropyridine-3-carboxamide (4). Compound 4 was synthesized following the standard procedures for preparing compound 3 from intermediates 2 (11.9 mg, 0.022 mmol) and 28b (17 mg, 0.022 mmol, 1.0 equiv). Compound 4 was obtained as a white solid (17.7 mg, yield 75%). ¹H NMR (600 MHz, CD₃OD): δ 8.94 (d, J = 1.2 Hz, 1H), 8.15 (s, 1H), 8.00 (d, J = 7.3 Hz, 2H), 7.91–7.82 (m, 1H), 7.52–7.33 (m, 6H), 7.26 (dd, J = 10.3, 8.6 Hz, 1H), 6.92 (s, 1H), 4.62 (s, 1H), 4.56 (dd, J = 9.4, 7.3 Hz, 1H), 4.50–4.41 (m, 2H), 4.32 (d, J = 15.5 Hz, 1H), 3.86 (d, J = 10.9 Hz, 1H), 3.81–3.74 (m, 2H), 3.74–3.69 (m, 1H), 3.69–3.59 (m, 3H), 3.58–3.49 (m, 3H), 3.37–3.32 (m, 2H), 2.98 (s, 5H), 2.56–2.49 (m, 2H), 2.44 (d, J = 1.2 Hz, 3H), 2.21 (dd, J = 13.1, 7.7 Hz, 1H), 2.11–2.03 (m, 1H), 1.44 (d, J = 6.5 Hz, 6H), 0.97 (s, 9H). HRMS (*m/z*): for C₅₄H₆₄F₄N₉O₈S⁺ [M + H]⁺ calcd, 1074.4529; found, 1074.4576.

N-(2'-Fluoro-5'-((2-(2-((S)-1-((2S,4R)-4-hydroxy-2-((4-(4-methylthiazol-5-yl)benzyl)carbamoyl)pyrrolidin-1-yl)-3,3-dimethyl-1-oxobutan-2-yl)amino)-2-oxoethoxy)ethoxy)ethyl)carbamoyl)-4-((3S,5R)-3,4,5-trimethylpiperazin-1-yl)-[1,1'-biphenyl]-3-yl)-6-oxo-4-(trifluoromethyl)-1,6-dihydropyridine-3-carboxamide (5). Compound 5 was synthesized following the standard procedures for preparing compound 3 from intermediates 2 (11.9 mg, 0.022 mmol) and 28c (13.5 mg, 0.022 mmol, 1.0 equiv). Compound 5 was obtained as a white solid (21.8 mg, yield 90%). ¹H NMR (600 MHz, CD₃OD): δ 8.95 (s, 1H), 8.14 (s, 1H), 8.01 (s, 1H), 7.94 (dd, J = 7.5, 2.4 Hz, 1H), 7.88–7.79 (m, 1H), 7.54–7.33 (m, 6H), 7.32–7.19 (m, 1H), 6.92 (s, 1H), 4.72 (s, 1H), 4.54–4.45 (m, 3H), 4.28 (d, J = 15.5 Hz, 1H), 4.05–3.88 (m, 2H), 3.84–3.77 (m, 1H), 3.73–3.63 (m, 6H), 3.61–3.50 (m, 5H), 3.36–3.32 (m, 4H), 2.98 (s, 3H), 2.46 (s, 3H), 2.26–2.15 (m, 1H), 2.13–1.99 (m, 1H), 1.44 (d, J = 6.4 Hz, 6H), 1.01 (s, 9H). HRMS (*m/z*): for C₅₅H₆₆F₄N₉O₉S⁺ [M + H]⁺ calcd, 1104.4635; found, 1104.4599.

N-(2'-Fluoro-5'-((2-(2-((S)-1-((2S,4R)-4-hydroxy-2-((4-(4-methylthiazol-5-yl)benzyl)carbamoyl)pyrrolidin-1-yl)-3,3-dimethyl-1-oxobutan-2-yl)amino)-3-oxopropoxy)ethoxy)ethyl)carbamoyl)-4-((3S,5R)-3,4,5-trimethylpiperazin-1-yl)-[1,1'-biphenyl]-3-yl)-6-oxo-4-(trifluoromethyl)-1,6-dihydropyridine-3-carboxamide (6). Compound 6 was synthesized following the standard procedures for preparing compound 3 from intermediates 2 (11.9 mg, 0.022 mmol) and 28d (17.9 mg, 0.022 mmol, 1.0 equiv). Compound 6 was obtained as a white solid (22.8 mg, yield 92%). ¹H NMR (600 MHz, CD₃OD): δ 8.97 (s, 1H), 8.15 (d, J = 2.0 Hz, 1H), 8.06–7.90 (m, 2H), 7.86–7.82 (m, 1H), 7.51–7.40 (m, 3H), 7.40–7.32 (m, 3H), 7.27 (dd, J = 10.3, 8.6 Hz, 1H), 6.92 (s, 1H), 4.63 (s, 1H), 4.59–4.45 (m, 3H), 4.33 (d, J = 15.5 Hz, 1H), 3.91–3.83 (m, 1H), 3.78 (dd, J = 10.9, 3.9 Hz, 1H), 3.74–3.47 (m, 12H), 3.36–3.30 (m, 2H), 3.02–2.92 (m, 5H), 2.53–2.38 (m, 5H), 2.23–2.17 (m, 1H), 2.10–2.01 (m, 1H), 1.44 (d, J = 6.5 Hz, 6H), 1.00 (s, 9H). HRMS (*m/z*): for C₅₆H₆₈F₄N₉O₉S⁺ [M + H]⁺ calcd, 1118.4791; found, 1118.4823.

N-(2'-Fluoro-5'-((S)-13-((2S,4R)-4-hydroxy-2-((4-(4-methylthiazol-5-yl)benzyl)carbamoyl)pyrrolidine-1-carbonyl)-14,14-dimethyl-11-oxo-3,6,9-trioxo-12-azapentadecyl)carbamoyl)-4-((3S,5R)-3,4,5-trimethylpiperazin-1-yl)-[1,1'-biphenyl]-3-yl)-6-oxo-4-(trifluoromethyl)-1,6-dihydropyridine-3-carboxamide (7). Compound 7 was synthesized following the standard procedures for preparing compound 3 from intermediates 2 (13 mg, 0.024 mmol) and 28e (20.3 mg, 0.024 mmol, 1.0 equiv). Compound 7 was obtained as a white solid (17.4 mg, yield 63%). ¹H NMR (600 MHz, CD₃OD): δ 8.95 (s, 1H), 8.15 (d, J = 2.1 Hz, 1H), 8.06–7.93 (m, 2H), 7.89–7.76 (m, 1H), 7.52–7.32 (m, 6H), 7.31–7.23 (m, 1H), 6.92 (s, 1H), 4.67 (s, 1H), 4.61–4.45 (m, 3H), 4.34 (d, J = 15.5 Hz, 1H), 4.01–3.89 (m, 2H), 3.88–3.74 (m, 2H), 3.69–3.47 (m, 14H), 3.36–3.34 (m, 1H), 3.33–3.32 (m, 1H), 3.09–2.92 (m, 5H), 2.46 (s, 3H), 2.28–2.16 (m, 1H), 2.13–2.02 (m, 1H), 1.44 (d, J = 6.5 Hz, 6H), 1.01 (s, 9H). HRMS (*m/z*): for C₅₇H₇₀F₄N₉O₁₀S⁺ [M + H]⁺ calcd, 1148.4897; found, 1148.4917.

N-(2'-Fluoro-5'-((S)-14-((2S,4R)-4-hydroxy-2-((4-(4-methylthiazol-5-yl)benzyl)carbamoyl)pyrrolidine-1-carbonyl)-15,15-dimethyl-12-oxo-3,6,9-trioxo-13-azahexadecyl)carbamoyl)-4-((3S,5R)-3,4,5-trimethylpiperazin-1-yl)-[1,1'-biphenyl]-3-yl)-6-oxo-4-(trifluoromethyl)-1,6-dihydropyridine-3-carboxamide (8). Compound 8 was synthesized following the standard procedures for preparing compound 3 from intermediates 2 (13 mg, 0.024 mmol) and 28f (20.7 mg, 0.024 mmol, 1.0 equiv). Compound 8 was obtained as a white solid (11.7 mg, yield 42%). ¹H NMR (600 MHz, CD₃OD): δ 8.97 (s, 1H), 8.15 (s, 1H), 8.07–7.94 (m, 2H), 7.85 (ddd, J = 8.5, 4.5, 2.4 Hz, 1H), 7.53–7.32 (m, 6H), 7.28 (dd, J = 10.3, 8.6 Hz, 1H), 6.92 (s, 1H), 4.62 (s, 1H), 4.58–4.45 (m, 3H), 4.34 (d, J = 15.5 Hz, 1H), 3.86 (d, J = 11.0 Hz, 1H), 3.77 (dd, J = 11.0, 3.9 Hz, 1H), 3.71–3.49 (m, 16H), 3.37–3.31 (m, 2H), 2.98 (s, 5H), 2.54–2.38 (m, 5H), 2.24–2.17 (m, 1H), 2.09–2.03 (m, 1H), 1.43 (d, J = 6.5 Hz, 6H), 1.00 (s, 9H). HRMS (*m/z*): for C₅₈H₇₂F₄N₉O₁₀S⁺ [M + H]⁺ calcd, 1162.5053; found, 1162.5043.

N-(2'-Fluoro-5'-((S)-17-((2S,4R)-4-hydroxy-2-((4-(4-methylthiazol-5-yl)benzyl)carbamoyl)pyrrolidine-1-carbonyl)-18,18-dimethyl-15-oxo-3,6,9,12-tetraoxo-16-azonadecyl)carbamoyl)-4-((3S,5R)-3,4,5-trimethylpiperazin-1-yl)-[1,1'-biphenyl]-3-yl)-6-oxo-4-(trifluoromethyl)-1,6-dihydropyridine-3-carboxamide (9). Compound 9 was synthesized following the standard procedures for preparing compound 3 from intermediates 2 (13 mg, 0.024 mmol) and 28g (17.1 mg, 0.024 mmol, 1.0 equiv). Compound 9 was obtained as a white solid (22.6 mg, yield 78%). ¹H NMR (600 MHz, CD₃OD): δ 9.03 (s, 1H), 8.16 (d, J = 1.9 Hz, 1H), 8.05–7.94 (m, 2H), 7.93–7.80 (m, 1H), 7.54–7.35 (m, 6H), 7.29 (dd, J = 10.3, 8.6 Hz, 1H), 6.92 (s, 1H), 4.63 (s, 1H), 4.60–4.46 (m, 3H), 4.35 (d, J = 15.5 Hz, 1H), 3.92–3.84 (m, 1H), 3.78 (dd, J = 11.0, 3.9 Hz, 1H), 3.74–3.47 (m, 20H), 3.38–3.30 (m, 2H), 3.05–2.91 (m, 5H), 2.58–2.50 (m, 1H), 2.50–2.39 (m, 4H), 2.24–2.18 (m, 1H), 2.10–2.04 (m, 1H), 1.44 (d, J = 6.5 Hz, 6H), 1.01 (s, 9H). HRMS (*m/z*): for C₆₀H₇₆F₄N₉O₁₁S⁺ [M + H]⁺ calcd, 1206.5316; found, 1206.5287.

N-(2'-Fluoro-5'-((S)-20-((2S,4R)-4-hydroxy-2-((4-(4-methylthiazol-5-yl)benzyl)carbamoyl)pyrrolidine-1-carbonyl)-21,21-dimethyl-18-oxo-3,6,9,12,15-pentaoxa-19-azadocosyl)carbamoyl)-4-((3S,5R)-3,4,5-trimethylpiperazin-1-yl)-[1,1'-biphenyl]-3-yl)-6-oxo-

4-(trifluoromethyl)-1,6-dihydropyridine-3-carboxamide (**10**). Compound **10** was synthesized following the standard procedures for preparing compound **3** from intermediates **2** (13 mg, 0.022 mmol) and **28h** (22.8 mg, 0.024 mmol, 1.0 equiv). Compound **10** was obtained as a white solid (15.3 mg, yield 51%). ¹H NMR (600 MHz, CD₃OD): δ 9.02 (s, 1H), 8.16 (d, *J* = 1.9 Hz, 1H), 8.06–7.97 (m, 2H), 7.93–7.82 (m, 1H), 7.54–7.36 (m, 6H), 7.29 (dd, *J* = 10.3, 8.6 Hz, 1H), 6.93 (s, 1H), 4.63 (s, 1H), 4.60–4.45 (m, 3H), 4.35 (d, *J* = 15.5 Hz, 1H), 3.87 (d, *J* = 11.2 Hz, 1H), 3.78 (dd, *J* = 11.0, 3.9 Hz, 1H), 3.74–3.48 (m, 24H), 3.38–3.32 (m, 2H), 2.98 (d, *J* = 3.0 Hz, 5H), 2.59–2.51 (m, 1H), 2.51–2.41 (m, 4H), 2.24–2.16 (m, 1H), 2.11–2.03 (m, 1H), 1.44 (d, *J* = 6.5 Hz, 6H), 1.02 (s, 9H). HRMS (*m/z*): for C₆₂H₈₀F₄N₉O₁₂S⁺ [M + H]⁺ calcd, 1250.5578; found, 1250.5534.

N-(2'-Fluoro-5'-((5-(((S)-1-((2S,4R)-4-hydroxy-2-((4-(4-methylthiazol-5-yl)benzyl)carbamoyl)pyrrolidin-1-yl)-3,3-dimethyl-1-oxobutan-2-yl)amino)-2-oxoethyl)carbamoyl)-4-((3S,5R)-3,4,5-trimethylpiperazin-1-yl)-[1,1'-biphenyl]-3-yl)-6-oxo-4-(trifluoromethyl)-1,6-dihydropyridine-3-carboxamide (**11**). Compound **11** was synthesized following the standard procedures for preparing compound **3** from intermediates **2** (13 mg, 0.024 mmol) and **29a** (17.2 mg, 0.024 mmol, 1.0 equiv). Compound **11** was obtained as a white solid (21.2 mg, yield 89%). ¹H NMR (400 MHz, CD₃OD): δ 8.99 (s, 1H), 8.15 (s, 1H), 8.04 (dd, *J* = 7.4, 2.4 Hz, 1H), 8.00 (s, 1H), 7.93–7.87 (m, 1H), 7.46 (dd, *J* = 10.0, 7.3 Hz, 3H), 7.41–7.34 (m, 3H), 7.29 (dd, *J* = 10.3, 8.6 Hz, 1H), 6.91 (s, 1H), 4.66 (s, 1H), 4.60–4.47 (m, 3H), 4.34 (d, *J* = 15.5 Hz, 1H), 4.10 (d, *J* = 11.7 Hz, 2H), 3.89 (d, *J* = 11.2 Hz, 1H), 3.79 (dd, *J* = 11.0, 3.8 Hz, 1H), 3.56–3.48 (m, 2H), 3.32–3.27 (m, 4H), 2.98 (s, 3H), 2.46 (s, 3H), 2.25–2.17 (m, 1H), 2.10–2.01 (m, 1H), 1.44 (d, *J* = 6.5 Hz, 6H), 1.04 (s, 9H). ¹³C NMR (101 MHz, CD₃OD): δ 174.44, 172.03, 171.33, 169.27, 165.27, 164.36, 162.90 (d, ¹*J*_{C-F} = 208.1 Hz, 1C, –*C-F), 161.15, 153.63, 147.65, 143.76, (q, ²*J*_{C-F} = 46.67 Hz, 1C), 141.57, 140.78, 133.62, 133.60, 131.84 (d, ³*J*_{C-F} = 3.56 Hz, 1C), 131.50 (d, ³*J*_{C-F} = 3.03 Hz, 1C), 130.75, 130.37 (2C), 130.04, 129.95, 129.62, 129.53, 129.47, 129.06 (2C), 128.15, 128.12, 123.39 (q, ¹*J*_{C-F} = 282.4 Hz, 1C, –*CF₃), 117.60, 117.36, 71.11, 62.45, 60.88, 59.07, 58.03, 57.61, 57.48, 57.27, 44.08, 43.67, 38.91, 37.40, 36.94, 26.98 (3C), 15.21, 15.15 (2C). *t*_R = 4.16 min, HRMS (*m/z*): for C₅₁H₅₈F₄N₉O₇S⁺ [M + H]⁺ calcd, 1016.4111; found, 1016.4124.

N-(2'-Fluoro-5'-((3-(((S)-1-((2S,4R)-4-hydroxy-2-((4-(4-methylthiazol-5-yl)benzyl)carbamoyl)pyrrolidin-1-yl)-3,3-dimethyl-1-oxobutan-2-yl)amino)-3-oxopropyl)carbamoyl)-4-((3S,5R)-3,4,5-trimethylpiperazin-1-yl)-[1,1'-biphenyl]-3-yl)-6-oxo-4-(trifluoromethyl)-1,6-dihydropyridine-3-carboxamide (**12**). Compound **12** was synthesized following the standard procedures for preparing compound **3** from intermediates **2** (13 mg, 0.024 mmol) and **29b** (17.5 mg, 0.024 mmol, 1.0 equiv). Compound **12** was obtained as a white solid (19 mg, yield 77%). ¹H NMR (600 MHz, CD₃OD): δ 8.96 (s, 1H), 8.14 (s, 1H), 8.07–7.93 (m, 2H), 7.89–7.77 (m, 1H), 7.50–7.24 (m, 7H), 6.92 (s, 1H), 4.61 (s, 1H), 4.58–4.46 (m, 3H), 4.33 (d, *J* = 15.5 Hz, 1H), 3.92 (d, *J* = 11.2 Hz, 1H), 3.78 (dd, *J* = 10.9, 3.9 Hz, 1H), 3.71–3.67 (m, 1H), 3.65–3.58 (m, 1H), 3.53 (q, *J* = 7.6, 5.4 Hz, 2H), 3.37–3.32 (m, 2H), 2.98 (d, *J* = 5.2 Hz, 5H), 2.67–2.54 (m, 2H), 2.46 (s, 3H), 2.23–2.16 (m, 1H), 2.09–2.02 (m, 1H), 1.44 (d, *J* = 6.5 Hz, 6H), 1.00 (s, 9H). HRMS (*m/z*): for C₅₂H₆₀F₄N₉O₇S⁺ [M + H]⁺ calcd, 1030.4267; found, 1030.4276.

N-(2'-Fluoro-5'-((4-(((S)-1-((2S,4R)-4-hydroxy-2-((4-(4-methylthiazol-5-yl)benzyl)carbamoyl)pyrrolidin-1-yl)-3,3-dimethyl-1-oxobutan-2-yl)amino)-4-oxobutyl)carbamoyl)-4-((3S,5R)-3,4,5-trimethylpiperazin-1-yl)-[1,1'-biphenyl]-3-yl)-6-oxo-4-(trifluoromethyl)-1,6-dihydropyridine-3-carboxamide (**13**). Compound **13** was synthesized following the standard procedures for preparing compound **3** from intermediates **2** (13 mg, 0.024 mmol) and **29c** (17.8 mg, 0.024 mmol, 1.0 equiv). Compound **13** was obtained as a white solid (18.7 mg, yield 75%). ¹H NMR (600 MHz, CD₃OD): δ 9.02 (s, 1H), 8.25–8.09 (m, 1H), 8.09–7.92 (m, 2H), 7.86 (ddd, *J* = 8.5, 4.5, 2.4 Hz, 1H), 7.55–7.34 (m, 6H), 7.29 (dd, *J* = 10.2, 8.6 Hz, 1H), 6.92 (s, 1H), 4.64–4.43 (m, 4H), 4.35 (d, *J* = 15.5 Hz, 1H), 3.90 (d, *J* = 11.0 Hz, 1H), 3.78 (dd, *J* = 11.0, 4.0 Hz, 1H), 3.60–3.50 (m, 2H), 3.41 (h, *J* = 6.7 Hz, 2H), 3.35–3.32 (m, 2H), 2.98 (s, 5H),

2.47 (s, 3H), 2.43–2.31 (m, 2H), 2.23–2.16 (m, 1H), 2.12–2.03 (m, 1H), 1.99–1.85 (m, 2H), 1.44 (d, *J* = 6.5 Hz, 6H), 1.03 (s, 9H). HRMS (*m/z*): for C₅₃H₆₂F₄N₉O₇S⁺ [M + H]⁺ calcd, 1044.4424; found, 1044.4445.

N-(2'-Fluoro-5'-((5-(((S)-1-((2S,4R)-4-hydroxy-2-((4-(4-methylthiazol-5-yl)benzyl)carbamoyl)pyrrolidin-1-yl)-3,3-dimethyl-1-oxobutan-2-yl)amino)-5-oxopentyl)carbamoyl)-4-((3S,5R)-3,4,5-trimethylpiperazin-1-yl)-[1,1'-biphenyl]-3-yl)-6-oxo-4-(trifluoromethyl)-1,6-dihydropyridine-3-carboxamide (**14**). Compound **14** was synthesized following the standard procedures for preparing compound **3** from intermediates **2** (13 mg, 0.024 mmol) and **29d** (13.6 mg, 0.024 mmol, 1.0 equiv). Compound **14** was obtained as a white solid (8.1 mg, yield 32%). ¹H NMR (600 MHz, CD₃OD): δ 8.96 (s, 1H), 8.15 (s, 1H), 8.05–7.93 (m, 2H), 7.88–7.82 (m, 1H), 7.55–7.22 (m, 7H), 6.93 (s, 1H), 4.63–4.41 (m, 4H), 4.34 (d, *J* = 15.5 Hz, 1H), 3.89 (d, *J* = 11.0 Hz, 1H), 3.78 (dd, *J* = 10.9, 3.9 Hz, 1H), 3.52 (d, *J* = 6.9 Hz, 2H), 3.40 (t, *J* = 6.7 Hz, 2H), 3.33 (t, *J* = 10.9 Hz, 2H), 2.98 (d, *J* = 7.6 Hz, 5H), 2.47 (s, 3H), 2.39–2.27 (m, 2H), 2.20 (dd, *J* = 13.2, 7.5 Hz, 1H), 2.13–2.03 (m, 1H), 1.75–1.60 (m, 4H), 1.44 (d, *J* = 6.5 Hz, 6H), 1.02 (s, 9H). HRMS (*m/z*): for C₅₄H₆₄F₄N₉O₇S⁺ [M + H]⁺ calcd, 1058.4580; found, 1058.4565.

N-(2'-Fluoro-5'-((7-(((S)-1-((2S,4R)-4-hydroxy-2-((4-(4-methylthiazol-5-yl)benzyl)carbamoyl)pyrrolidin-1-yl)-3,3-dimethyl-1-oxobutan-2-yl)amino)-7-oxoheptyl)carbamoyl)-4-((3S,5R)-3,4,5-trimethylpiperazin-1-yl)-[1,1'-biphenyl]-3-yl)-6-oxo-4-(trifluoromethyl)-1,6-dihydropyridine-3-carboxamide (**15**). Compound **15** was synthesized following the standard procedures for preparing compound **3** from intermediates **2** (13 mg, 0.024 mmol) and **29e** (13.9 mg, 0.024 mmol, 1.0 equiv). Compound **15** was obtained as a white solid (15.9 mg, yield 63%). ¹H NMR (600 MHz, CD₃OD): δ 8.99 (s, 1H), 8.15 (s, 1H), 8.03–7.95 (m, 2H), 7.88–7.70 (m, 1H), 7.64–7.35 (m, 6H), 7.28 (dd, *J* = 10.2, 8.6 Hz, 1H), 6.92 (s, 1H), 4.63–4.44 (m, 4H), 4.34 (d, *J* = 15.5 Hz, 1H), 3.89 (dd, *J* = 11.1, 2.1 Hz, 1H), 3.78 (dd, *J* = 11.0, 3.9 Hz, 1H), 3.60–3.48 (m, 2H), 3.42–3.37 (m, 2H), 3.34–3.30 (m, 2H), 3.06–2.93 (m, 5H), 2.47 (s, 3H), 2.36–2.25 (m, 2H), 2.22–2.17 (m, 1H), 2.13–2.02 (m, 1H), 1.72–1.56 (m, 4H), 1.48–1.34 (m, 8H), 1.00 (s, 9H). HRMS (*m/z*): for C₅₅H₆₆F₄N₉O₇S⁺ [M + H]⁺ calcd, 1072.4737; found, 1072.4713.

N-(2'-Fluoro-5'-((8-(((S)-1-((2S,4R)-4-hydroxy-2-((4-(4-methylthiazol-5-yl)benzyl)carbamoyl)pyrrolidin-1-yl)-3,3-dimethyl-1-oxobutan-2-yl)amino)-8-oxooctyl)carbamoyl)-4-((3S,5R)-3,4,5-trimethylpiperazin-1-yl)-[1,1'-biphenyl]-3-yl)-6-oxo-4-(trifluoromethyl)-1,6-dihydropyridine-3-carboxamide (**16**). Compound **16** was synthesized following the standard procedures for preparing compound **3** from intermediates **2** (13 mg, 0.024 mmol) and **29f** (14.3 mg, 0.024 mmol, 1.0 equiv). Compound **16** was obtained as a white solid (12.6 mg, yield 48%). ¹H NMR (600 MHz, CD₃OD): δ 8.97 (s, 1H), 8.14 (s, 1H), 8.01 (s, 1H), 7.96 (dd, *J* = 7.4, 2.4 Hz, 1H), 7.86–7.80 (m, 1H), 7.49–7.41 (m, 3H), 7.43–7.35 (m, 3H), 7.27 (dd, *J* = 10.3, 8.5 Hz, 1H), 6.93 (s, 1H), 4.62 (s, 1H), 4.60–4.46 (m, 3H), 4.34 (d, *J* = 15.5 Hz, 1H), 3.90 (d, *J* = 11.0 Hz, 1H), 3.79 (dd, *J* = 11.0, 3.9 Hz, 1H), 3.53–3.50 (m, 2H), 3.42–3.30 (m, 4H), 3.04–2.93 (m, 5H), 2.47 (s, 3H), 2.33–2.17 (m, 3H), 2.11–2.04 (m, 1H), 1.66–1.60 (m, 4H), 1.55–1.30 (m, 10H), 1.00 (s, 9H). HRMS (*m/z*): for C₅₆H₆₈F₄N₉O₇S⁺ [M + H]⁺ calcd, 1086.4893; found, 1086.4910.

N-(2'-Fluoro-5'-((10-(((S)-1-((2S,4R)-4-hydroxy-2-((4-(4-methylthiazol-5-yl)benzyl)carbamoyl)pyrrolidin-1-yl)-3,3-dimethyl-1-oxobutan-2-yl)amino)-10-oxodecyl)carbamoyl)-4-((3S,5R)-3,4,5-trimethylpiperazin-1-yl)-[1,1'-biphenyl]-3-yl)-6-oxo-4-(trifluoromethyl)-1,6-dihydropyridine-3-carboxamide (**17**). Compound **17** was synthesized following the standard procedures for preparing compound **7** from intermediates **2** (13 mg, 0.024 mmol) and **29g** (19.2 mg, 0.024 mmol, 1.0 equiv). Compound **17** was obtained as a white solid (16.7 mg, yield 63%). ¹H NMR (600 MHz, CD₃OD): δ 8.96 (s, 1H), 8.15 (s, 1H), 8.02–7.93 (m, 2H), 7.86–7.80 (m, 1H), 7.50–7.34 (m, 6H), 7.27 (dd, *J* = 10.3, 8.6 Hz, 1H), 6.92 (s, 1H), 4.62 (s, 1H), 4.59–4.46 (m, 3H), 4.35 (d, *J* = 15.4 Hz, 1H), 3.89 (d, *J* = 11.0 Hz, 1H), 3.79 (dd, *J* = 10.9, 3.9 Hz, 1H), 3.58–3.54 (m, 2H), 3.40–3.33 (m, 4H), 2.98 (d, *J* = 5.5 Hz, 5H), 2.47 (s, 3H), 2.33–2.16 (m, 3H), 2.10–2.02 (m, 1H), 1.70–1.52 (m, 4H), 1.44 (d, *J* = 6.5 Hz,

6H), 1.42–1.30 (m, 6H), 1.01 (s, 9H). HRMS (*m/z*): for C₅₇H₇₀F₄N₉O₇S⁺ [M + H]⁺ calcd, 1100.5050; found, 1100.5076.

N-(2'-Fluoro-5'-((1-(((S)-1-((2S,4R)-4-hydroxy-2-((4-(4-methylthiazol-5-yl)benzyl)carbamoyl)pyrrolidin-1-yl)-3,3-dimethyl-1-oxobutan-2-yl)amino)-11-oxoundecyl)carbamoyl)-4-((3S,5R)-3,4,5-trimethylpiperazin-1-yl)-[1,1'-biphenyl]-3-yl)-6-oxo-4-(trifluoromethyl)-1,6-dihydropyridine-3-carboxamide (18). Compound 18 was synthesized following the standard procedures for preparing compound 3 from intermediates 2 (13 mg, 0.024 mmol) and 29h (14.9 mg, 0.024 mmol, 1.0 equiv). Compound 18 was obtained as a white solid (19.1 mg, yield 71%). ¹H NMR (600 MHz, CD₃OD): δ 8.99 (s, 1H), 8.16–8.13 (m, 1H), 8.01 (s, 1H), 7.97 (dd, *J* = 7.4, 2.4 Hz, 1H), 7.86–7.80 (m, 1H), 7.52–7.34 (m, 6H), 7.31–7.24 (m, 1H), 6.93 (s, 1H), 4.62 (s, 1H), 4.60–4.46 (m, 3H), 4.35 (d, *J* = 15.5 Hz, 1H), 3.92–3.87 (m, 1H), 3.79 (dd, *J* = 11.0, 3.9 Hz, 1H), 3.57–3.47 (m, 2H), 3.40–3.31 (m, 4H), 2.98 (d, *J* = 3.9 Hz, 5H), 2.47 (s, 3H), 2.33–2.17 (m, 3H), 2.11–2.03 (m, 1H), 1.66–1.55 (m, 4H), 1.44 (d, *J* = 6.5 Hz, 6H), 1.39–1.32 (m, 8H), 1.02 (s, 9H). HRMS (*m/z*): for C₅₈H₇₂F₄N₉O₇S⁺ [M + H]⁺ calcd, 1114.5206; found, 1114.5243.

N-(2'-Fluoro-5'-((1-(((S)-1-((2S,4R)-4-hydroxy-2-((4-(4-methylthiazol-5-yl)benzyl)carbamoyl)pyrrolidin-1-yl)-3,3-dimethyl-1-oxobutan-2-yl)amino)-10-oxodecyl)carbamoyl)-4-((3S,5R)-3,4,5-trimethylpiperazin-1-yl)-[1,1'-biphenyl]-3-yl)-6-oxo-4-(trifluoromethyl)-1,6-dihydropyridine-3-carboxamide (19). Compound 19 was synthesized following the standard procedures for preparing compound 3 from intermediates 2 (13 mg, 0.024 mmol) and 29i (19.8 mg, 0.024 mmol, 1.0 equiv). Compound 19 was obtained as a white solid (12.6 mg, yield 33%). ¹H NMR (600 MHz, CD₃OD): δ 8.99 (s, 1H), 8.15 (s, 1H), 8.03–7.94 (m, 2H), 7.83 (ddd, *J* = 8.7, 4.6, 2.4 Hz, 1H), 7.51–7.45 (m, 2H), 7.48–7.35 (m, 4H), 7.31–7.25 (m, 1H), 6.93 (s, 1H), 4.62 (s, 1H), 4.60–4.47 (m, 3H), 4.35 (d, *J* = 15.4 Hz, 1H), 3.89 (d, *J* = 11.0 Hz, 1H), 3.79 (dd, *J* = 10.9, 3.9 Hz, 1H), 3.54–3.51 (m, 2H), 3.40–3.30 (m, 4H), 3.06–2.90 (m, 5H), 2.48 (s, 3H), 2.32–2.17 (m, 3H), 2.11–2.03 (m, 1H), 1.61 (dd, *J* = 16.1, 8.9 Hz, 4H), 1.44 (d, *J* = 6.5 Hz, 6H), 1.41–1.22 (m, 10H), 1.02 (s, 9H). HRMS (*m/z*): for C₅₉H₇₄F₄N₉O₇S⁺ [M + H]⁺ calcd, 1128.5363; found, 1128.5341.

N-(2'-Fluoro-5'-((1-(((S)-1-((2S,4R)-4-hydroxy-2-((4-(4-methylthiazol-5-yl)benzyl)carbamoyl)pyrrolidin-1-yl)-3,3-dimethyl-1-oxobutan-2-yl)amino)-11-oxoundecyl)carbamoyl)-4-((3S,5R)-3,4,5-trimethylpiperazin-1-yl)-[1,1'-biphenyl]-3-yl)-6-oxo-4-(trifluoromethyl)-1,6-dihydropyridine-3-carboxamide (20). Compound 20 was synthesized following the standard procedures for preparing compound 3 from intermediates 2 (13 mg, 0.024 mmol) and 29j (15.6 mg, 0.024 mmol, 1.0 equiv). Compound 20 was obtained as a white solid (16 mg, yield 58%). ¹H NMR (600 MHz, CD₃OD): δ 8.94 (s, 1H), 8.17–8.13 (m, 1H), 8.03–7.94 (m, 2H), 7.84 (ddd, *J* = 8.5, 4.6, 2.4 Hz, 1H), 7.51–7.35 (m, 6H), 7.28 (dd, *J* = 10.3, 8.6 Hz, 1H), 6.93 (s, 1H), 4.62 (s, 1H), 4.59–4.47 (m, 3H), 4.35 (d, *J* = 15.5 Hz, 1H), 3.89 (d, *J* = 11.0 Hz, 1H), 3.79 (dd, *J* = 11.0, 3.9 Hz, 1H), 3.52 (s, 2H), 3.40–3.30 (m, 4H), 2.98 (s, 5H), 2.47 (s, 3H), 2.32–2.17 (m, 3H), 2.09–2.05 (m, 1H), 1.65–1.56 (m, 4H), 1.44 (d, *J* = 6.5 Hz, 6H), 1.43–1.20 (m, 12H), 1.02 (s, 9H). HRMS (*m/z*): for C₆₀H₇₆F₄N₉O₇S⁺ [M + H]⁺ calcd, 1142.5519; found, 1142.5487.

N-(3'-((4-(2-(8-(2-((2-(2,6-Dioxopiperidin-3-yl)-1,3-dioxoisindolin-4-yl)oxy)acetamido)octanamido)ethyl)piperazin-1-yl)methyl)-4-(4-methylpiperazin-1-yl)-[1,1'-biphenyl]-3-yl)-6-oxo-4-(trifluoromethyl)-1,6-dihydropyridine-3-carboxamide (21). Compound 21 was synthesized following the standard procedures for preparing compound 3 from intermediates 38 (63.4 mg, 0.11 mmol) and 34 (50.2 mg, 0.11 mmol, 1.0 equiv). Compound 21 was obtained as a white solid (79.5 mg, 69%). ¹H NMR (600 MHz, CD₃OD): δ 8.27 (d, *J* = 2.1 Hz, 1H), 8.06 (s, 1H), 7.83–7.62 (m, 3H), 7.57–7.44 (m, 4H), 7.39 (dd, *J* = 8.4, 6.9 Hz, 2H), 6.93 (s, 1H), 5.13 (dd, *J* = 12.9, 5.5 Hz, 1H), 4.73 (s, 2H), 4.34 (s, 2H), 3.63 (d, *J* = 11.7 Hz, 2H), 3.55–3.40 (m, 10H), 3.37 (s, 2H), 3.35–3.30 (m, 3H), 3.24–3.14 (m, 4H), 2.98 (s, 3H), 2.95–2.83 (m, 1H), 2.79–2.69 (m, 2H), 2.67 (s, 1H), 2.21 (t, *J* = 7.6 Hz, 2H), 2.18–2.10 (m, 1H), 1.63–1.51 (m, 4H), 1.41–1.27 (m, 6H). ¹³C NMR (151 MHz, CD₃OD): δ 176.09, 173.20, 170.09, 168.34, 166.91, 166.34, 163.87, 162.50, 154.81,

142.33, 140.99, 140.08 (q, ²*J*_{C-F} = 33.0 Hz, 1C, –*C–F), 138.37, 137.32, 136.86, 133.43, 132.64, 130.91, 129.59, 129.48, 128.99, 127.86, 124.43, 122.07, 121.02 (q, ¹*J*_{C-F} = 273.0 Hz, 1C, –*C–F), 120.99, 120.20, 119.22 (d, ³*J*_{C-F} = 3.0 Hz, 1C, –*C–F), 117.74, 116.54, 113.02, 67.85, 63.73, 60.13, 56.32, 53.77, 53.59, 49.64, 49.18, 49.10, 48.91, 48.48, 42.31, 39.05, 38.71, 35.40, 34.39, 30.80, 28.71 (2C), 28.54, 26.24, 25.11, 22.22. HRMS (*m/z*): for C₅₄H₆₄F₃N₁₀O₉⁺ [M + H]⁺ calcd, 1053.4804; found, 1053.4811.

N-(3'-((4-(2-(8-(2-((2-(1-Methyl-2,6-dioxopiperidin-3-yl)-1,3-dioxoisindolin-4-yl)oxy)acetamido)octanamido)ethyl)piperazin-1-yl)methyl)-4-(4-methylpiperazin-1-yl)-[1,1'-biphenyl]-3-yl)-6-oxo-4-(trifluoromethyl)-1,6-dihydropyridine-3-carboxamide (22). Compound 22 was synthesized following the standard procedures for preparing compound 3 from intermediates 38 (29.6 mg, 0.05 mmol) and 35 (24.2 mg, 0.05 mmol, 1.0 equiv). Compound 22 was obtained as a white solid (40.2 mg, 75%). ¹H NMR (600 MHz, CD₃OD): δ 8.28 (d, *J* = 2.1 Hz, 1H), 8.05 (s, 1H), 7.84–7.77 (m, 2H), 7.77–7.70 (m, 1H), 7.59–7.51 (m, 3H), 7.48 (d, *J* = 7.6 Hz, 1H), 7.40 (dd, *J* = 16.0, 8.4 Hz, 2H), 6.94 (s, 1H), 5.16 (dd, *J* = 13.0, 5.4 Hz, 1H), 4.76 (s, 2H), 4.32 (s, 2H), 3.63 (d, *J* = 11.8 Hz, 2H), 3.51 (t, *J* = 5.9 Hz, 2H), 3.47–3.35 (m, 14H), 3.22–3.07 (m, 7H), 2.98 (s, 3H), 2.95–2.86 (m, 2H), 2.76–2.57 (m, 1H), 2.21 (t, *J* = 7.6 Hz, 2H), 2.16–2.08 (m, 1H), 1.69–1.51 (m, 4H), 1.41–1.25 (m, 6H). ¹³C NMR (151 MHz, CD₃OD): δ 176.01, 172.17, 169.82, 168.38, 166.90, 166.37, 163.87, 162.50, 154.88, 142.31, 140.99, 140.08 (q, ²*J*_{C-F} = 33.0 Hz, 1C, –*C–F), 138.36, 137.41, 136.86, 133.47, 132.64, 131.15, 129.54, 129.45, 128.94, 127.80, 124.42, 122.02 (q, ¹*J*_{C-F} = 273.0 Hz, 1C, –*C–F), 122.11, 120.97, 120.27, 119.24 (d, ³*J*_{C-F} = 3.0 Hz, 1C, –*C–F), 117.80, 116.56, 113.03, 67.92, 60.17, 56.33, 53.75, 53.60, 49.82, 49.77, 49.28, 48.92, 48.46, 42.30, 38.69, 35.38, 34.48, 31.07, 28.73, 28.69, 28.50, 26.23 (2C), 26.01 (2C), 25.11, 21.45. HRMS (*m/z*): for C₅₅H₆₆F₃N₁₀O₉⁺ [M + H]⁺ calcd, 1067.4961; found, 1067.4968.

N-(3'-((4-(2-(5-(2-((2-(2,6-Dioxopiperidin-3-yl)-1,3-dioxoisindolin-4-yl)oxy)acetamido)pentanamido)ethyl)piperazin-1-yl)methyl)-4-(4-methylpiperazin-1-yl)-[1,1'-biphenyl]-3-yl)-6-oxo-4-(trifluoromethyl)-1,6-dihydropyridine-3-carboxamide (23). Compound 23 was synthesized following the standard procedures for preparing compound 3 from intermediates 38 (62.7 mg, 0.105 mmol) and 36 (45.3 mg, 0.105 mmol, 1.0 equiv). Compound 23 was obtained as a white solid (72 mg, 68%). ¹H NMR (600 MHz, CD₃OD): δ 8.26 (d, *J* = 2.2 Hz, 1H), 8.05 (s, 1H), 7.87–7.69 (m, 3H), 7.58–7.52 (m, 2H), 7.49 (dd, *J* = 7.6, 4.7 Hz, 2H), 7.37 (dd, *J* = 8.4, 4.8 Hz, 2H), 6.93 (s, 1H), 5.12 (dd, *J* = 12.9, 5.5 Hz, 1H), 4.73 (s, 2H), 4.39 (s, 2H), 3.62 (d, *J* = 11.8 Hz, 2H), 3.59–3.40 (m, 10H), 3.38–3.31 (m, 5H), 3.29–3.26 (m, 1H), 3.23–3.15 (m, 4H), 2.98 (s, 3H), 2.92–2.80 (m, 1H), 2.80–2.63 (m, 2H), 2.26 (t, *J* = 7.3 Hz, 2H), 2.19–2.07 (m, 1H), 1.71–1.51 (m, 4H). ¹³C NMR (151 MHz, CD₃OD): δ 175.63, 173.15, 170.15, 168.46, 166.88, 166.39, 163.88, 162.51, 154.92, 142.38, 140.08 (q, ²*J*_{C-F} = 31.5 Hz, 1C, –*C–F), 140.13, 138.38, 137.24, 136.86, 133.43, 132.60, 130.39, 129.70, 129.52, 129.11, 128.00, 124.45, 122.02 (q, ¹*J*_{C-F} = 276.0 Hz, 1C, –*C–F), 122.14, 120.97, 120.32, 119.24 (d, ³*J*_{C-F} = 3.0 Hz, 1C, –*C–F), 117.73, 116.56, 113.00, 67.95, 60.03, 56.31, 53.76, 53.58 (2C), 49.43, 49.16, 48.90, 48.47, 42.31, 38.38, 34.84, 34.30, 30.77 (2C), 28.36 (2C), 22.31, 22.20. HRMS (*m/z*): for C₅₁H₅₈F₃N₁₀O₉⁺ [M + H]⁺ calcd, 1011.4335; found, 1011.4329.

N-(3'-((4-(2-(5-(2-((2-(1-Methyl-2,6-dioxopiperidin-3-yl)-1,3-dioxoisindolin-4-yl)oxy)acetamido)pentanamido)ethyl)piperazin-1-yl)methyl)-4-(4-methylpiperazin-1-yl)-[1,1'-biphenyl]-3-yl)-6-oxo-4-(trifluoromethyl)-1,6-dihydropyridine-3-carboxamide (24). Compound 24 was synthesized following the standard procedures for preparing compound 3 from intermediates 38 (71.6 mg, 0.12 mmol) and 37 (51.4 mg, 0.12 mmol, 1.0 equiv). Compound 24 was obtained as a white solid (97.8 mg, 80%). ¹H NMR (600 MHz, CD₃OD): δ 8.26 (d, *J* = 2.3 Hz, 1H), 8.06 (s, 1H), 7.86–7.65 (m, 3H), 7.59–7.52 (m, 2H), 7.52–7.44 (m, 2H), 7.38 (dd, *J* = 8.4, 5.6 Hz, 2H), 6.92 (s, 1H), 5.14 (dd, *J* = 13.0, 5.4 Hz, 1H), 4.75 (s, 2H), 4.37 (s, 2H), 3.63 (d, *J* = 11.7 Hz, 2H), 3.56–3.38 (m, 8H), 3.37 (s, 8H), 3.26–3.15 (m, 4H), 3.11 (s, 3H), 2.98 (s, 3H), 2.93–2.81 (m, 2H), 2.76–2.58 (m, 1H), 2.25 (t, *J* = 7.3 Hz, 2H), 2.16–2.06 (m, 1H), 1.72–1.50 (m,

4H). ^{13}C NMR (151 MHz, CD_3OD): δ 175.50, 172.15, 169.86, 168.45, 166.90, 166.35, 163.86, 162.49, 154.94, 142.39, 140.99, 140.08 (q, $^2J_{\text{C-F}} = 31.5$ Hz, 1C, $-\text{*C-F}$), 138.40, 137.26, 136.86, 133.45, 132.63, 130.64, 129.64, 129.49, 129.07, 127.93, 124.44, 122.02 (q, $^1J_{\text{C-F}} = 276.0$ Hz, 1C, $-\text{*C-F}$), 122.15, 120.97, 120.27, 119.23 (d, $^3J_{\text{C-F}} = 3.0$ Hz, 1C, $-\text{*C-F}$), 117.70, 116.54, 113.00, 67.91, 60.06, 56.27, 53.78, 53.58, 49.81, 49.52, 49.07, 48.89, 48.48 (2C), 42.31, 38.38, 34.84, 34.33, 31.07, 28.39, 26.03 (2C), 22.33, 21.43. HRMS (m/z): for $\text{C}_{52}\text{H}_{60}\text{F}_3\text{N}_{10}\text{O}_9^+$ [$\text{M} + \text{H}$] $^+$ calcd, 1025.4481; found, 1025.4486.

N-(5'-((7-(2-((2-(2,6-Dioxopiperidin-3-yl)-1,3-dioxoisindolin-4-yl)oxy)acetamido)heptyl)carbamoyl)-2'-fluoro-4-((3*S*,5*R*)-3,4,5-trimethylpiperazin-1-yl)-[1,1'-biphenyl]-3-yl)-6-oxo-4-(trifluoromethyl)-1,6-dihydropyridine-3-carboxamide (25). Compound 25 was synthesized following the standard procedures for preparing compound 3 from intermediates 2 (27.3 mg, 0.05 mmol) and 40 (27.2 mg, 0.05 mmol, 1.0 equiv). Compound 25 was obtained as a white solid (34.6 mg, 71%). ^1H NMR (400 MHz, CD_3OD): δ 8.16 (s, 1H), 8.04 (s, 1H), 7.97 (dd, $J = 7.6, 2.1$ Hz, 1H), 7.87–7.80 (m, 1H), 7.80–7.72 (m, 1H), 7.54–7.44 (m, 2H), 7.42–7.34 (m, 2H), 7.33–7.20 (m, 1H), 6.93 (s, 1H), 5.21–5.08 (m, 1H), 4.73 (d, $J = 1.8$ Hz, 2H), 3.64–3.48 (m, 2H), 3.34–3.27 (m, 4H), 3.01 (d, $J = 1.8$ Hz, 3H), 2.92–2.66 (m, 3H), 2.18–2.10 (m, 1H), 2.06 (s, 6H), 1.68–1.52 (m, 4H), 1.51–1.35 (m, 10H). HRMS (m/z): for $\text{C}_{49}\text{H}_{53}\text{F}_4\text{N}_8\text{O}_9^+$ [$\text{M} + \text{H}$] $^+$ calcd, 973.3866; found, 973.3869.

N-(2'-Fluoro-5'-((7-(2-((1-methyl-2,6-dioxopiperidin-3-yl)-1,3-dioxoisindolin-4-yl)oxy)acetamido)heptyl)carbamoyl)-4-((3*S*,5*R*)-3,4,5-trimethylpiperazin-1-yl)-[1,1'-biphenyl]-3-yl)-6-oxo-4-(trifluoromethyl)-1,6-dihydropyridine-3-carboxamide (26). Compound 26 was synthesized following the standard procedures for preparing compound 3 from intermediates 2 (54.7 mg, 0.1 mmol) and 41 (45.8 mg, 0.1 mmol, 1.0 equiv). Compound 26 was obtained as a white solid (64.8 mg, 66%). ^1H NMR (400 MHz, CD_3OD): δ 8.16 (s, 1H), 8.04 (s, 1H), 7.97 (dd, $J = 7.7, 2.3$ Hz, 1H), 7.86–7.80 (m, 1H), 7.79–7.72 (m, 1H), 7.47 (q, $J = 4.1$ Hz, 2H), 7.38 (dd, $J = 8.4, 6.3$ Hz, 2H), 7.27 (t, $J = 9.5$ Hz, 1H), 6.92 (s, 1H), 5.15 (dd, $J = 13.1, 5.3$ Hz, 1H), 4.73 (s, 2H), 3.57 (t, $J = 8.2$ Hz, 2H), 3.34–3.24 (m, 4H), 3.12 (d, $J = 1.8$ Hz, 3H), 3.00 (s, 3H), 2.98–2.75 (m, 2H), 2.73–2.60 (m, 1H), 2.18–2.09 (m, 1H), 2.08–1.98 (m, 6H), 1.67–1.52 (m, 4H), 1.52–1.42 (m, 4H), 1.42–1.29 (m, 6H). HRMS (m/z): for $\text{C}_{50}\text{H}_{55}\text{F}_4\text{N}_8\text{O}_9^+$ [$\text{M} + \text{H}$] $^+$ calcd, 987.4023; found, 987.4034.

N-(2'-Fluoro-5'-((2-((5-((2*R*,4*S*)-4-hydroxy-2-((4-(4-methylthiazol-5-yl)benzyl)carbamoyl)pyrrolidin-1-yl)-3,3-dimethyl-1-oxobutan-2-yl)amino)-2-oxoethyl)carbamoyl)-4-((3*S*,5*R*)-3,4,5-trimethylpiperazin-1-yl)-[1,1'-biphenyl]-3-yl)-6-oxo-4-(trifluoromethyl)-1,6-dihydropyridine-3-carboxamide (27). Compound 27 was synthesized following the standard procedures for preparing compound 3 from intermediates 2 (18.3 mg, 0.033 mmol) and 44 52 (16.3 mg, 0.02 mmol, 1.0 equiv). Compound 20 was obtained as a white solid (29.2 mg, 89%). ^1H NMR (400 MHz, CD_3OD): δ 9.13 (s, 1H), 8.12 (s, 1H), 8.01 (d, $J = 8.1$ Hz, 1H), 7.94 (dd, $J = 7.4, 2.4$ Hz, 1H), 7.83–7.79 (m, 1H), 7.41–7.37 (m, 1H), 7.33 (d, $J = 8.3$ Hz, 1H), 7.30 (s, 4H), 7.23 (dd, $J = 10.3, 8.5$ Hz, 1H), 6.92 (s, 1H), 4.54 (t, $J = 7.5$ Hz, 1H), 4.52–4.48 (m, 1H), 4.47–4.39 (m, 2H), 4.29 (d, $J = 15.5$ Hz, 1H), 4.08 (s, 2H), 3.97 (q, $J = 5.5, 5.1$ Hz, 2H), 3.72 (dd, $J = 10.9, 3.3$ Hz, 1H), 3.56–3.46 (m, 2H), 3.02–2.92 (m, 6H), 2.43 (s, 3H), 2.27–2.21 (m, 1H), 2.13–2.09 (m, 1H), 1.44 (dd, $J = 6.2, 4.1$ Hz, 6H), 1.09 (s, 9H). ^{13}C NMR (101 MHz, CD_3OD): δ 174.25, 172.27, 168.93, 165.19, 162.84 (d, $^1J_{\text{C-F}} = 216.14$ Hz, 1C, $-\text{*C-F}$), 152.85, 148.84, 143.61, 141.55, 141.22, 140.02 (q, $^2J_{\text{C-F}} = 47.47$ Hz, 1C), 133.64, 131.70 (d, $^3J_{\text{C-F}} = 3.0$ Hz, 1C), 131.42 (d, $^3J_{\text{C-F}} = 3.0$ Hz, 1C), 131.34, 130.57, 130.29 (2C), 129.95, 129.86, 129.65, 129.50, 129.36, 128.79 (2C), 128.07 (d, $^2J_{\text{C-F}} = 16.16$ Hz, 1C), 125.75, 123.36 (q, $^1J_{\text{C-F}} = 288.9$ Hz, 1C), 120.62, 117.57, 117.33, 114.39, 70.52, 62.43, 60.96, 60.10, 60.00, 57.60, 56.91, 43.81, 43.43, 39.09, 37.43, 35.69, 27.00 (3C), 15.80, 15.14 (2C). $t_{\text{R}} = 4.31$ min, HRMS (m/z): for $\text{C}_{51}\text{H}_{57}\text{F}_4\text{N}_9\text{O}_7\text{S}^+$ [$\text{M} + \text{H}$] $^+$ calcd, 1016.4111; found, 1016.4111.

8-(2-((2-(2,6-Dioxopiperidin-3-yl)-1,3-dioxoisindolin-4-yl)oxy)acetamido)octanoic Acid (34). To a solution of intermediate 30 (99.6 mg, 0.3 mmol) in DMSO (1 mL) were added commercially

available linker 32 (64.5 mg, 0.3 mmol, 1.0 equiv), EDCI (86.4 mg, 0.45 mmol, 1.5 equiv), HOAt (61.2 mg, 0.45 mmol, 1.5 equiv), and NMM (91 mg, 0.9 mmol, 3.0 equiv). After stirring overnight at rt, the resulting mixture was purified by preparative HPLC (10–100% methanol/0.1% TFA in H_2O) to afford the Boc-protected intermediate. This intermediate was dissolved in TFA/DCM (1 mL/1 mL), and the mixture was stirred at rt for 30 min. The solvent was removed under reduced pressure, and the resulting mixture was purified by preparative HPLC (10–100% methanol/0.1% TFA in H_2O) to afford compound 34 as a white solid (50.2 mg, yield 36%). ^1H NMR (600 MHz, CD_3OD): δ 7.80 (dd, $J = 8.4, 7.3$ Hz, 1H), 7.53 (d, $J = 7.3$ Hz, 1H), 7.43 (d, $J = 8.5$ Hz, 1H), 5.15 (dd, $J = 12.8, 5.4$ Hz, 1H), 4.76 (s, 2H), 3.35 (d, $J = 21.9$ Hz, 2H), 2.98–2.88 (m, 1H), 2.83–2.65 (m, 2H), 2.28 (t, $J = 7.4$ Hz, 2H), 2.21–2.09 (m, 1H), 1.66–1.50 (m, 4H), 1.44–1.26 (m, 6H). ESI (m/z): [$\text{M} + \text{H}$] $^+$, 474.5.

8-(2-((2-(1-Methyl-2,6-dioxopiperidin-3-yl)-1,3-dioxoisindolin-4-yl)oxy)acetamido)octanoic Acid (35). Compound 35 was synthesized following the standard procedures for preparing compound 34 from intermediates 31 (50 mg, 0.029 mmol) and 32 (31 mg, 0.029 mmol, 1.0 equiv). Compound 35 was obtained as a white solid (24.2 mg, 29%). ^1H NMR (600 MHz, CD_3OD): δ 7.88–7.77 (m, 1H), 7.54 (d, $J = 7.3$ Hz, 1H), 7.44 (d, $J = 8.4$ Hz, 1H), 5.18 (dd, $J = 13.0, 5.4$ Hz, 1H), 4.77 (s, 2H), 3.35–3.28 (m, 2H), 3.17 (s, 3H), 2.99–2.86 (m, 2H), 2.74–2.71 (m, 1H), 2.28 (t, $J = 7.4$ Hz, 2H), 2.18–2.10 (m, 1H), 1.62–1.58 (m, 4H), 1.39–1.31 (m, 6H). ESI (m/z): [$\text{M} + \text{H}$] $^+$, 488.8.

5-(2-((2-(2,6-Dioxopiperidin-3-yl)-1,3-dioxoisindolin-4-yl)oxy)acetamido)pentanoic Acid (36). Compound 36 was synthesized following the standard procedures for preparing compound 34 from intermediates 30 (22.9 mg, 0.07 mmol) and 33 (14.5 mg, 0.07 mmol, 1.0 equiv). Compound 36 was obtained as a white solid (23.9 mg, 79%). ^1H NMR (600 MHz, $\text{DMSO}-d_6$): δ 12.00 (s, 1H), 11.12 (s, 1H), 7.98 (t, $J = 5.8$ Hz, 1H), 7.81 (dd, $J = 8.5, 7.3$ Hz, 1H), 7.50 (d, $J = 7.3$ Hz, 1H), 7.39 (d, $J = 8.5$ Hz, 1H), 5.12 (dd, $J = 12.9, 5.4$ Hz, 1H), 3.17 (s, 2H), 3.15 (q, $J = 6.6$ Hz, 2H), 2.90 (ddd, $J = 17.1, 13.9, 5.5$ Hz, 1H), 2.70–2.53 (m, 2H), 2.22 (t, $J = 7.1$ Hz, 2H), 2.08–2.01 (m, 1H), 1.58–1.34 (m, 4H). ESI (m/z): [$\text{M} + \text{H}$] $^+$, 432.6.

5-(2-((2-(1-Methyl-2,6-dioxopiperidin-3-yl)-1,3-dioxoisindolin-4-yl)oxy)acetamido)pentanoic Acid (37). Compound 37 was synthesized following the standard procedures for preparing compound 34 from intermediates 31 (50 mg, 0.14 mmol) and 33 (30 mg, 0.14 mmol, 1.0 equiv). Compound 37 was obtained as a white solid (51.4 mg, 83%). ^1H NMR (600 MHz, CD_3OD): δ 7.70 (dd, $J = 8.5, 7.3$ Hz, 1H), 7.42 (d, $J = 7.3$ Hz, 1H), 7.33 (d, $J = 8.4$ Hz, 1H), 5.07 (dd, $J = 13.0, 5.4$ Hz, 1H), 4.67 (s, 2H), 3.26–3.21 (m, 2H), 3.06 (s, 3H), 2.86–2.73 (m, 2H), 2.65–2.58 (m, 1H), 2.23 (t, $J = 7.1$ Hz, 2H), 2.07–2.01 (m, 1H), 1.62–1.42 (m, 4H). ESI (m/z): [$\text{M} + \text{H}$] $^+$, 446.8.

N-(7-Aminoheptyl)-2-((2-(2,6-dioxopiperidin-3-yl)-1,3-dioxoisindolin-4-yl)oxy)acetamide (40). Compound 40 was synthesized following the standard procedures for preparing compound 34 from intermediates 30 (66.4 mg, 0.2 mmol) and 39 (92.2 mg, 0.4 mmol, 2.0 equiv). Compound 40 was obtained as a white solid (55.4 mg, 64%). ^1H NMR (400 MHz, CD_3OD): δ 7.82–7.80 (m, 1H), 7.56 (dd, $J = 7.5, 1.7$ Hz, 1H), 7.46 (dd, $J = 8.5, 1.7$ Hz, 1H), 5.19–5.16 (m, 1H), 4.78 (d, $J = 1.8$ Hz, 2H), 3.37 (d, $J = 1.7$ Hz, 2H), 2.95 (dd, $J = 11.1, 5.4$ Hz, 4H), 2.75–2.71 (m, 1H), 2.24v–2.11 (m, 1H), 1.67–1.63 (m, 4H), 1.42–1.38 (m, 6H). ESI (m/z): [$\text{M} + \text{H}$] $^+$, 445.6.

N-(7-Aminoheptyl)-2-((2-(1-methyl-2,6-dioxopiperidin-3-yl)-1,3-dioxoisindolin-4-yl)oxy)acetamide (41). Compound 41 was synthesized following the standard procedures for preparing compound 34 from intermediates 31 (80 mg, 0.23 mmol) and 39 (106 mg, 0.46 mmol, 2.0 equiv). Compound 41 was obtained as a white solid (45.8 mg, 43%). ^1H NMR (400 MHz, CD_3OD): δ 7.83–7.81 (m, 1H), 7.55 (dd, $J = 7.5, 1.7$ Hz, 1H), 7.45 (dd, $J = 8.5, 1.7$ Hz, 1H), 5.18 (ddd, $J = 12.8, 5.4, 1.8$ Hz, 1H), 4.78 (d, $J = 1.8$ Hz, 2H), 3.37 (d, $J = 1.7$ Hz, 2H), 3.17 (d, $J = 1.7$ Hz, 3H), 2.93 (dd, $J = 11.1,$

5.4 Hz, 4H), 2.76–2.72 (m, 1H), 2.22–2.10 (m, 1H), 1.66–1.61 (m, 4H), 1.42–1.40 (m, 6H). ESI (m/z): $[M + H]^+$, 459.5.

(2*R*,4*S*)-1-((*S*)-2-(2-Aminoacetamido)-3,3-dimethylbutanoyl)-4-hydroxy-*N*-(4-(4-methylthiazol-5-yl)benzyl)pyrrolidine-2-carboxamide (**44**). Compound **44** was synthesized following the standard procedures for preparing compound **34** from intermediates **42** (215 mg, 0.5 mmol) and **43** (175 mg, 1.0 mmol, 2.0 equiv). Compound **44** was obtained as a white solid (136 mg, 56%). $^1\text{H NMR}$ (600 MHz, CD_3OD): δ 8.97 (s, 1H), 7.54–7.38 (m, 4H), 4.67 (s, 1H), 4.63–4.52 (m, 3H), 4.38 (d, $J = 15.4$ Hz, 1H), 3.99–3.93 (m, 1H), 3.87–3.70 (m, 3H), 2.51 (s, 3H), 2.29–2.24 (m, 1H), 2.14–2.09 (m, 1H), 1.09 (s, 9H). HRMS m/z : for $\text{C}_{24}\text{H}_{34}\text{N}_5\text{O}_4\text{S}^+$ $[M + H]^+$ calcd, 488.2326; found, 488.2322.

Cell Lines and Tissue Culture. Human leukemia MV4;11 cells (American Tissue Culture Collection [ATCC], CRL-9591) were cultured in the RPMI 1640 base medium supplemented with 10% FBS and 1% penicillin/streptomycin. Human PDAC cells used in the work include BxPC-3 (ATCC, CRL-1687), HPAF-II (ATCC, CRL-1997), PANC-1 (ATCC, CRL-1469), and Panc 10.05 (ATCC, CRL-2547) cells, which were cultured in RPMI 1640 supplemented with 10% FBS and 1% penicillin/streptomycin. The MIA PaCa-2 (ATCC, CRL-1420) PDAC cells were cultured in DMEM supplemented with 10% FBS and 1% penicillin/streptomycin.

Authentication of cell line identities, including those of parental and derived lines, was ensured by the tissue culture facility affiliated to the UNC Lineberger Comprehensive Cancer Center with genetic signature profiling and fingerprinting analysis. Every 1–2 months, a routine examination of cell lines in culture for any possible mycoplasma contamination was performed using commercially available detection kits (Lonza).

Preparation of Proteins for ITC Studies. For the expression of the full-length N-terminal His-tagged WDR5 (Uniprot accession number P61964), the pET28-LIC-WDR5 vector was obtained from Addgene (plasmid number 25489). The plasmid was transformed into *Escherichia coli* BL21 (DE3) cells and grown at 37 °C until the culture reached an OD_{600} of ~ 2.0 . The temperature was then reduced to 18 °C, and the expression was induced by the addition of 0.5 mM IPTG, followed by incubation for 16 h. The cells were then resuspended in a lysis buffer (50 mM Tris pH 7.5, 500 mM NaCl, 5% glycerol, 0.01% IGEPAL, 25 mM imidazole, and 5 mM 2-mercaptoethanol) in the presence of Pierce protease inhibitor tablets, EDTA-free (Thermo Fisher), and 1 mM PMSF. The cells were lysed by sonication, clarified by centrifugation, the filtered supernatant was loaded onto a HisTrap HP affinity column (GE Healthcare), and the protein was eluted using an imidazole gradient ranging from 25 to 250 mM. The fractions containing WDR5 protein were concentrated and subjected to size exclusion chromatography by HiLoad 26/600 Superdex 200 (GE Healthcare), pre-equilibrated with 20 mM HEPES pH 7.5, 150 mM NaCl, and 2 mM TCEP.

For the expression of the His-tagged VCB complex, a plasmid containing pVHL_{54–213} (P40337) with an N-terminal His tag and a TEV protease cleavable site was cotransformed with a pCDF duet plasmid containing EloB_{1–104} (Q15370) and EloC_{1–112} (Q15369) into *E. coli* BL21 (DE3) cells. The cells were grown at 37 °C until OD_{600} reached 2.0, and then the temperature was reduced to 18 °C and IPTG was added to a final concentration of 0.4 mM. The cells were harvested at 16 h post induction and resuspended in a lysis buffer (50 mM Tris pH 7.5, 500 mM NaCl, 5% glycerol, 0.01% IGEPAL, 25 mM imidazole, and 5 mM 2-mercaptoethanol) in the presence of Pierce protease inhibitor tablets, EDTA-free (Thermo Fisher), and 1 mM PMSF. The clarified lysate after centrifugation was loaded onto a 5 mL HisTrap HP affinity column and purified with an imidazole gradient. The protein was further purified by gel filtration using HiLoad 26/600 Superdex 200. The final purified protein was flash frozen in liquid nitrogen and stored at -80 °C in 50 mM Tris pH 7.5, 150 mM NaCl, and 2 mM TCEP.

Antibodies and Immunoblotting. Total cell lysate was used for Western blots as previously described.⁵⁹ The following primary antibodies were used in the study: WDR5 (Santa Cruz, sc-393080), tubulin (Cell Signaling Technology, 2144), and vinculin (Cell

Signaling, 13901S). Blots were imaged using fluorescence-labeled secondary antibodies on ChemiDoc Imaging Systems.

Cell Proliferation Assay by Counting. $1\text{--}5 \times 10^5/\text{mL}$ of cells were seeded in triplicate in the 24-well plates. Compounds were added at a range of concentrations indicated in the study. Mediums with fresh compounds were changed every 2 days. Cells were passaged with dilution to keep cell density under $1 \times 10^6/\text{mL}$ at all times. Cells were counted by an automated cell counter (Biorad, TC10) every 2 days. 50% of maximal growth inhibition (GI_{50}) values were calculated using GraphPad Prism software using a nonlinear regression analysis, and the mean \pm SEM was calculated from triplicated treatment data.

MTS (3-(4,5-Dimethylthiazol-2-yl)-5-(3-carboxymethoxyphenyl)-2-(4-sulfophenyl)-2H-tetrazolium) Assay. Pancreatic cancer cells were seeded at a density of 500 or 1000 cells per well in 96-well plates and incubated with the indicated compounds at different time points. Fresh medium with compound was changed every 2 days. At each time point, MTS reagent (Promega) was added to the cell culture medium and incubated for 0.5–2 h under standard culture conditions. Then, the plates were briefly shaken and subjected to measure absorbance at 490 nm using a CYTATION-5 imaging reader (BioTek).

Proteomics Profiling. Four million MIA PaCa-2 cells were seeded in each of the 10 cm plates, and after the cells became adhered to the dish bottom, they were treated with DMSO or 1.5 μM of compound **11** for 2.5 h. Cells were then harvested and washed three times in $1 \times$ PBS, followed by lysis in the lysis buffer (8 M urea, 50 mM Tris-HCl, and pH 8.0) with the use of the tip probe sonicator (Fisher) to help the lysis process. The resulting lysis samples were centrifuged at maximum speed for 15 min in a refrigerated microfuge to completely remove cell debris. The protein concentration was measured by a Bradford assay, and the samples were then frozen at -80 °C until further analysis. For MS analysis, 200 μg of each sample was reduced with 5 mM DTT at 56 °C for 30 min, alkylated with 15 mM iodoacetamide at room temperature in the dark for 45 min, then diluted to 1 M urea with 50 mM ammonium bicarbonate (pH 7.8). The samples were digested with LysC (Wako) and trypsin (Promega) at a 1:50 ratio overnight at 37 °C. After desalting using Waters SepPak C18 cartridges, a Pierce colorimetric peptide quantitation assay was performed to determine the digested peptide concentration. Then, 50 μg of each sample was labeled with an individual tandem mass tag (TMT) 10plex reagent at room temperature with shaking for 2 h. The reactions were quenched and combined into a single multiplexed sample. A 100 μg aliquot of the mixed sample was fractionated into 8 fractions using the Pierce high pH reversed phase fractionation spin columns. Peptide fractions were analyzed on the Easy nLC 1200-QEactive HF (carried out in the UNC Proteomics Core). Raw data were searched against a reviewed Uniprot human database (containing 20,245 sequences) using Andromeda within MaxQuant software (version 1.6.2.10). Proteins were quantified using TMT intensities, and the data were further analyzed in Perseus, Excel, and GraphPad.

Mouse PK Study. Compound **11** (in its HCl salt form) was dissolved in a solution formulation of 5% NMP, 5% solutol HS-15, and 90% normal saline. Six male Swiss albino mice were administered intraperitoneally with a solution formulation of compound **11** at 75 mg/kg. Blood samples (approximately 60 μL) were collected under light isoflurane anesthesia from a set of three mice at 0.5, 1, 2, 4, 8, and 12 h. Plasma was harvested by centrifugation of blood and stored at -70 ± 10 °C until analysis. The plasma concentration–time of compound **11** was used for the PK analysis. Plasma samples were quantified by the fit-for-purpose LC-MS/MS method (LLOQ: 5.03 ng/mL). PK analysis was performed using GraphPad Prism software in the form of nonlinear regression analysis. The compound concentrations in plasma at each time point are the average values from three test mice. Error bars represent \pm SEM.

Mutagenesis on Human WDR5 and Generation of Stable Cell Lines with WDR5 Mutants. The WDR5 WT and mutant nucleotide sequences were modified from p3x Flag-CMV-14-WDR5 (Addgene plasmid #59974). Point mutations were introduced by

PCR using the Q5 site-directed mutagenesis kit (New England E0554S). The mutagenic primers used followed the same procedures described in previous reports.⁴⁸ PCRs for single lysine to arginine mutations were run for 25 cycles of 30 s at 98 °C and 1 min at 68 to 74 °C, 2 min 30 s at 72 °C, followed by 10 min at 72 °C. The resulting mutant plasmids were verified by Sanger sequencing. The WDR5 WT and mutant PCR fragments with 3X flag-tag were cloned into lentiviral TetO-Puro vectors. The lentiviral TetO-WDR5-Puro vectors were utilized to transduce HEK293T cells to generate inducible/stable cell lines that overexpress WDR5 WT, K32R, and K296R mutants. For lentivirus production, HEK293T cells were seeded in DMEM medium supplemented with 10% fetal bovine serum. Plasmid DNA vectors containing human WDR5 WT and its mutants were transfected using lipofectamine (3000) according to the manufacturer's protocol. After 48 and 72 h of transfection, lentivirus packaging cell supernatant was collected and concentrated using the Lenti-X concentrator (Takara, 631232). Concentrated lentivirus was quantified using Lenti-GoStix Plus (Takara 631280) and applied to HEK293T cells for 24 h in the presence of 5 µg/mL Polybrene (Sigma). WDR5 overexpression was induced by the addition of 1 µg/mL doxycycline to the medium. After puromycin selection for 4 days, the stable cell lines were utilized for further experiments. Cell lysates were collected at 72 h after the stable cell lines were treated with the indicated concentrations of MS67. Supernatants were run on 4–12% gradient SDS-PAGE gels and transferred to a nitrocellulose membrane (BioRad) using the Trans-Blot Turbo system (BioRad). Membranes were probed with WDR5 (SantaCruz, G-9) and vinculin (Cell Signaling, 13901S) antibodies. Western blot images were detected using the LI-COR machine (LI-COR Biosciences). The images were cropped at specific protein bands of interest using Image Studio (LI-COR Biosciences) to improve the clarity of the data presentation.

Statistics and Reproducibility. Experimental data are presented as the mean ± SD or SEM of three independent experiments unless otherwise noted. Statistical analysis was performed using an unpaired two-sided Student's *t*-test for comparing two sets of data with an assumed normal distribution. The results for immunoblotting are representative of at least two biologically independent experiments unless otherwise noted. All statistical analyses and visualizations were performed using GraphPad (Prism v8.4.2) or Excel.

■ ASSOCIATED CONTENT

SI Supporting Information

The Supporting Information is available free of charge at <https://pubs.acs.org/doi/10.1021/acs.jmedchem.3c01521>.

Molecular formula strings for all compounds (CSV)
Effects of compounds **21** and **25** on inducing WDR5 degradation in MV4;11 cells; inverse ITC titrations of VCB into **11** and WDR5-**11** complex and of WDR5 into **11**; inverse ITC titrations of VCB and WDR5 into **27**; effects of compound **11** on inducing WDR5 degradation in MIA PaCa-2 cells; Western blotting verification of the WDR5 degradation induced by compound **11** in MIA PaCa-2 cell lysates for proteomic studies; and ¹H NMR, ¹³C NMR, and HPLC spectra of compounds **11** and **27** (PDF)

■ AUTHOR INFORMATION

Corresponding Authors

Gang Greg Wang – Lineberger Comprehensive Cancer Center, University of North Carolina at Chapel Hill School of Medicine, Chapel Hill, North Carolina 27599, United States; Department of Biochemistry and Biophysics, University of North Carolina at Chapel Hill, Chapel Hill, North Carolina 27599, United States; Department of Pharmacology, University of North Carolina at Chapel Hill School of

Medicine, Chapel Hill, North Carolina 27599, United States; Duke Cancer Institute, Department of Pathology, and Department of Pharmacology and Cancer Biology, Duke University School of Medicine, Durham, North Carolina 27710, United States; Email: greg.wang@duke.edu

Jian Jin – Mount Sinai Center for Therapeutics Discovery, Icahn School of Medicine at Mount Sinai, New York, New York 10029, United States; Departments of Pharmacological Sciences and Oncological Sciences, Tisch Cancer Institute, Icahn School of Medicine at Mount Sinai, New York, New York 10029, United States; orcid.org/0000-0002-2387-3862; Email: jian.jin@mssm.edu

Authors

Xufen Yu – Mount Sinai Center for Therapeutics Discovery, Icahn School of Medicine at Mount Sinai, New York, New York 10029, United States; Departments of Pharmacological Sciences and Oncological Sciences, Tisch Cancer Institute, Icahn School of Medicine at Mount Sinai, New York, New York 10029, United States; orcid.org/0000-0001-7794-7890

Dongxu Li – Lineberger Comprehensive Cancer Center, University of North Carolina at Chapel Hill School of Medicine, Chapel Hill, North Carolina 27599, United States; Department of Biochemistry and Biophysics, University of North Carolina at Chapel Hill, Chapel Hill, North Carolina 27599, United States; orcid.org/0000-0003-1440-7293

Jithesh Kottur – Mount Sinai Center for Therapeutics Discovery, Icahn School of Medicine at Mount Sinai, New York, New York 10029, United States; Departments of Pharmacological Sciences and Oncological Sciences, Tisch Cancer Institute, Icahn School of Medicine at Mount Sinai, New York, New York 10029, United States

Huen Suk Kim – Mount Sinai Center for Therapeutics Discovery, Icahn School of Medicine at Mount Sinai, New York, New York 10029, United States; Departments of Pharmacological Sciences and Oncological Sciences, Tisch Cancer Institute, Icahn School of Medicine at Mount Sinai, New York, New York 10029, United States

Laura E. Herring – Department of Pharmacology, University of North Carolina at Chapel Hill School of Medicine, Chapel Hill, North Carolina 27599, United States; orcid.org/0000-0003-4496-7312

Yao Yu – Lineberger Comprehensive Cancer Center, University of North Carolina at Chapel Hill School of Medicine, Chapel Hill, North Carolina 27599, United States; Department of Biochemistry and Biophysics, University of North Carolina at Chapel Hill, Chapel Hill, North Carolina 27599, United States; Duke Cancer Institute, Department of Pathology, and Department of Pharmacology and Cancer Biology, Duke University School of Medicine, Durham, North Carolina 27710, United States

Ling Xie – Department of Biochemistry and Biophysics, University of North Carolina at Chapel Hill, Chapel Hill, North Carolina 27599, United States

Xiaoping Hu – Mount Sinai Center for Therapeutics Discovery, Icahn School of Medicine at Mount Sinai, New York, New York 10029, United States; Departments of Pharmacological Sciences and Oncological Sciences, Tisch Cancer Institute, Icahn School of Medicine at Mount Sinai, New York, New York 10029, United States

Xian Chen – Department of Biochemistry and Biophysics, University of North Carolina at Chapel Hill, Chapel Hill, North Carolina 27599, United States

Ling Cai – Lineberger Comprehensive Cancer Center, University of North Carolina at Chapel Hill School of Medicine, Chapel Hill, North Carolina 27599, United States; Duke Cancer Institute and Department of Pathology, Duke University School of Medicine, Durham, North Carolina 27710, United States

Jing Liu – Mount Sinai Center for Therapeutics Discovery, Icahn School of Medicine at Mount Sinai, New York, New York 10029, United States; Departments of Pharmacological Sciences and Oncological Sciences, Tisch Cancer Institute, Icahn School of Medicine at Mount Sinai, New York, New York 10029, United States

Aneel K. Aggarwal – Departments of Pharmacological Sciences and Oncological Sciences, Tisch Cancer Institute, Icahn School of Medicine at Mount Sinai, New York, New York 10029, United States

Complete contact information is available at:

<https://pubs.acs.org/10.1021/acs.jmedchem.3c01521>

Author Contributions

○X.Y., D.L., and J.K. contributed equally to this work.

Notes

The authors declare the following competing financial interest(s): J.J., G.G.W., J.L., D.L., and X.Y. are inventors of a patent application filed by the Icahn School of Medicine at Mount Sinai. J.J. is a cofounder and equity shareholder in Cullgen, Inc., a scientific cofounder and scientific advisory board member of Onsero Therapeutics, Inc., and a consultant for Cullgen, Inc., EpiCypher, Inc., Accent Therapeutics, Inc., and Tavotek Biotherapeutics, Inc. The Jin laboratory received research funds from the Celgene Corporation, Levo Therapeutics, Inc., Cullgen, Inc., and Cullinan Oncology, Inc.

ACKNOWLEDGMENTS

This work was supported in part by the grants R01CA268384 (to J.J. and G.G.W.) and R35GM131780 (to A.K.A.) from the U.S. National Institutes of Health (NIH) and an endowed professorship from the Icahn School of Medicine at Mount Sinai (to A.K.A.). This work utilized the NMR spectrometer systems at Mount Sinai acquired with funding from the NIH's SIG grants 1S10OD025132 and 1S10OD028504.

ABBREVIATIONS USED

ASH2L, absent small homeotic-2-like protein; CRBN, cereblon; EDCI, 1-ethyl-3-(3-(dimethylamino)propyl)-carbodiimide; H3K4me2 and H3K4me3, histone H3 lysine 4 di- and trimethylation; HOAT, 1-hydroxy-7-azabenzotriazole; IKZF1, ikaros; IP, intraperitoneal; ITC, isothermal titration calorimetry; MLL1, mixed lineage leukemia 1; MLL-r, mixed lineage leukemia rearranged; MOA, mechanism of action; MS, mass spectrometry; PDAC, pancreatic ductal adenocarcinoma; PEG, polyethylene glycol; PK, pharmacokinetic; POI, protein of interest; PPIs, protein–protein interactions; PROTAC, proteolysis targeting chimera; RBBP5, retinoblastoma-binding protein 5; SAR, structure–activity relationship; TMT, tandem mass tags; TPD, targeting protein degradation; UPS, ubiquitin proteasome system; VHL, von Hippel-Lindau; WB, Western blotting; WBM, WDR5 binding motif; WDR5, WD repeat domain 5; WIN, WDR5 interaction; WT, wild-type

REFERENCES

- (1) Guarnaccia, A. D.; Tansey, W. P. Moonlighting with WDR5: A Cellular Multitasker. *J. Clin. Med.* **2018**, *7* (2), 21.
- (2) Trievel, R. C.; Shilatifard, A. WDR5, a complexed protein. *Nat. Struct. Mol. Biol.* **2009**, *16* (7), 678–680.
- (3) Schapira, M.; Tyers, M.; Torrent, M.; Arrowsmith, C. H. WD40 repeat domain proteins: a novel target class? *Nat. Rev. Drug Discovery* **2017**, *16* (11), 773–786.
- (4) Jain, B. P.; Pandey, S. WD40 Repeat Proteins: Signalling Scaffold with Diverse Functions. *Protein J.* **2018**, *37* (5), 391–406.
- (5) Han, Z.; Guo, L.; Wang, H.; Shen, Y.; Deng, X. W.; Chai, J. Structural basis for the specific recognition of methylated histone H3 lysine 4 by the WD-40 protein WDR5. *Mol. Cell* **2006**, *22* (1), 137–144.
- (6) Couture, J. F.; Collazo, E.; Trievel, R. C. Molecular recognition of histone H3 by the WD40 protein WDR5. *Nat. Struct. Mol. Biol.* **2006**, *13* (8), 698–703.
- (7) Dharmarajan, V.; Lee, J. H.; Patel, A.; Skalnik, D. G.; Cosgrove, M. S. Structural basis for WDR5 interaction (Win) motif recognition in human SET1 family histone methyltransferases. *J. Biol. Chem.* **2012**, *287* (33), 27275–27289.
- (8) Carugo, A.; Genovese, G.; Seth, S.; Nezi, L.; Rose, J. L.; Bossi, D.; Cicalese, A.; Shah, P. K.; Viale, A.; Pettazoni, P. F.; et al. In Vivo Functional Platform Targeting Patient-Derived Xenografts Identifies WDR5-Myc Association as a Critical Determinant of Pancreatic Cancer. *Cell Rep.* **2016**, *16* (1), 133–147.
- (9) Alicea-Velazquez, N. L.; Shinsky, S. A.; Loh, D. M.; Lee, J. H.; Skalnik, D. G.; Cosgrove, M. S. Targeted Disruption of the Interaction between WD-40 Repeat Protein 5 (WDR5) and Mixed Lineage Leukemia (MLL)/SET1 Family Proteins Specifically Inhibits MLL1 and SETd1A Methyltransferase Complexes. *J. Biol. Chem.* **2016**, *291* (43), 22357–22372.
- (10) Thomas, L. R.; Adams, C. M.; Wang, J.; Weissmiller, A. M.; Creighton, J.; Lorey, S. L.; Liu, Q.; Fesik, S. W.; Eischen, C. M.; Tansey, W. P. Interaction of the oncoprotein transcription factor MYC with its chromatin cofactor WDR5 is essential for tumor maintenance. *Proc. Natl. Acad. Sci. U.S.A.* **2019**, *116* (50), 25260–25268.
- (11) Ge, Z.; Song, E. J.; Kawasaki, Y. I.; Li, J.; Dovat, S.; Song, C. WDR5 high expression and its effect on tumorigenesis in leukemia. *Oncotarget* **2016**, *7* (25), 37740–37754.
- (12) Ge, Z.; Song, E.; Li, J.; Dovat, S.; Song, C. Clinical Significance of WDR5 High Expression and Its Effect on Tumorigenesis in Adult Leukemia. *Blood* **2015**, *126* (23), 3657.
- (13) Wu, M.; Shu, H. B. MLL1/WDR5 complex in leukemogenesis and epigenetic regulation. *Chin. J. Cancer* **2011**, *30* (4), 240–246. From NLM Medline
- (14) Dai, X.; Guo, W.; Zhan, C.; Liu, X.; Bai, Z.; Yang, Y. WDR5 Expression Is Prognostic of Breast Cancer Outcome. *PLoS One* **2015**, *10* (9), No. e0124964.
- (15) Cai, W. L.; Chen, J. F.; Chen, H.; Wingrove, E.; Kurley, S. J.; Chan, L. H.; Zhang, M.; Arnal-Estape, A.; Zhao, M.; Balabaki, A.; et al. Human WDR5 promotes breast cancer growth and metastasis via KMT2-independent translation regulation. *Elife* **2022**, *11*, No. e78163.
- (16) Malek, R.; Gajula, R. P.; Williams, R. D.; Nghiem, B.; Simons, B. W.; Nugent, K.; Wang, H.; Taparra, K.; Lemtiri-Chlieh, G.; Yoon, A. R.; et al. TWIST1-WDR5-Hottip Regulates Hoxa9 Chromatin to Facilitate Prostate Cancer Metastasis. *Cancer Res.* **2017**, *77* (12), 3181–3193.
- (17) Sun, W.; Guo, F.; Liu, M. Up-regulated WDR5 promotes gastric cancer formation by induced cyclin D1 expression. *J. Cell. Biochem.* **2018**, *119* (4), 3304–3316.
- (18) Tan, X.; Chen, S.; Wu, J.; Lin, J.; Pan, C.; Ying, X.; Pan, Z.; Qiu, L.; Liu, R.; Geng, R.; et al. PI3K/AKT-mediated upregulation of WDR5 promotes colorectal cancer metastasis by directly targeting ZNF407. *Cell Death Dis.* **2017**, *8* (3), No. e2686.
- (19) Chen, X.; Xie, W.; Gu, P.; Cai, Q.; Wang, B.; Xie, Y.; Dong, W.; He, W.; Zhong, G.; Lin, T.; et al. Upregulated WDR5 promotes

- proliferation, self-renewal and chemoresistance in bladder cancer via mediating H3K4 trimethylation. *Sci. Rep.* **2015**, *5*, 8293.
- (20) Sun, Y.; Bell, J. L.; Carter, D.; Gherardi, S.; Poulos, R. C.; Milazzo, G.; Wong, J. W.; Al-Awar, R.; Tee, A. E.; Liu, P. Y.; et al. WDR5 Supports an N-Myc Transcriptional Complex That Drives a Protumorigenic Gene Expression Signature in Neuroblastoma. *Cancer Res.* **2015**, *75* (23), 5143–5154.
- (21) Han, Q. L.; Zhang, X. L.; Ren, P. X.; Mei, L. H.; Lin, W. H.; Wang, L.; Cao, Y.; Li, K.; Bai, F. Discovery, evaluation and mechanism study of WDR5-targeted small molecular inhibitors for neuroblastoma. *Acta Pharmacol. Sin.* **2023**, *44* (4), 877–887.
- (22) Chen, X.; Xu, J.; Wang, X.; Long, G.; You, Q.; Guo, X. Targeting WD Repeat-Containing Protein 5 (WDR5): A Medicinal Chemistry Perspective. *J. Med. Chem.* **2021**, *64* (15), 10537–10556.
- (23) Thomas, L. R.; Adams, C. M.; Fesik, S. W.; Eischen, C. M.; Tansey, W. P. Targeting MYC through WDR5. *Mol. Cell Oncol.* **2020**, *7* (2), 1709388.
- (24) Karatas, H.; Townsend, E. C.; Cao, F.; Chen, Y.; Bernard, D.; Liu, L.; Lei, M.; Dou, Y.; Wang, S. High-affinity, small-molecule peptidomimetic inhibitors of MLL1/WDR5 protein-protein interaction. *J. Am. Chem. Soc.* **2013**, *135* (2), 669–682.
- (25) Cao, F.; Townsend, E. C.; Karatas, H.; Xu, J.; Li, L.; Lee, S.; Liu, L.; Chen, Y.; Ouillette, P.; Zhu, J.; et al. Targeting MLL1 H3K4 methyltransferase activity in mixed-lineage leukemia. *Mol. Cell* **2014**, *53* (2), 247–261.
- (26) Karatas, H.; Li, Y.; Liu, L.; Ji, J.; Lee, S.; Chen, Y.; Yang, J.; Huang, L.; Bernard, D.; Xu, J.; et al. Discovery of a Highly Potent, Cell-Permeable Macrocyclic Peptidomimetic (MM-589) Targeting the WD Repeat Domain 5 Protein (WDR5)-Mixed Lineage Leukemia (MLL) Protein-Protein Interaction. *J. Med. Chem.* **2017**, *60* (12), 4818–4839.
- (27) Senisterra, G.; Wu, H.; Allali-Hassani, A.; Wasney, G. A.; Barsyte-Lovejoy, D.; Dombrowski, L.; Dong, A.; Nguyen, K. T.; Smil, D.; Bolshan, Y.; et al. Small-molecule inhibition of MLL activity by disruption of its interaction with WDR5. *Biochem. J.* **2013**, *449* (1), 151–159.
- (28) Grebien, F.; Vedadi, M.; Getlik, M.; Giambruno, R.; Grover, A.; Avellino, R.; Skucha, A.; Vittori, S.; Kuznetsova, E.; Smil, D.; et al. Pharmacological targeting of the Wdr5-MLL interaction in C/EBP α N-terminal leukemia. *Nat. Chem. Biol.* **2015**, *11* (8), 571–578.
- (29) Zhu, J.; Sammons, M. A.; Donahue, G.; Dou, Z.; Vedadi, M.; Getlik, M.; Barsyte-Lovejoy, D.; Al-awar, R.; Katona, B. W.; Shilatifard, A.; et al. Gain-of-function p53 mutants co-opt chromatin pathways to drive cancer growth. *Nature* **2015**, *525* (7568), 206–211.
- (30) Getlik, M.; Smil, D.; Zepeda-Velazquez, C.; Bolshan, Y.; Poda, G.; Wu, H.; Dong, A.; Kuznetsova, E.; Marcellus, R.; Senisterra, G.; et al. Structure-Based Optimization of a Small Molecule Antagonist of the Interaction Between WD Repeat-Containing Protein 5 (WDR5) and Mixed-Lineage Leukemia 1 (MLL1). *J. Med. Chem.* **2016**, *59* (6), 2478–2496.
- (31) Li, D. D.; Chen, W. L.; Wang, Z. H.; Xie, Y. Y.; Xu, X. L.; Jiang, Z. Y.; Zhang, X. J.; You, Q. D.; Guo, X. K. High-affinity small molecular blockers of mixed lineage leukemia 1 (MLL1)-WDR5 interaction inhibit MLL1 complex H3K4 methyltransferase activity. *Eur. J. Med. Chem.* **2016**, *124*, 480–489.
- (32) Wang, F.; Jeon, K. O.; Salovich, J. M.; Macdonald, J. D.; Alvarado, J.; Gogliotti, R. D.; Phan, J.; Olejniczak, E. T.; Sun, Q.; Wang, S.; et al. Discovery of Potent 2-Aryl-6,7-dihydro-5 H-pyrrolo[1,2-a]imidazoles as WDR5-WIN-Site Inhibitors Using Fragment-Based Methods and Structure-Based Design. *J. Med. Chem.* **2018**, *61* (13), 5623–5642.
- (33) Aho, E. R.; Wang, J.; Gogliotti, R. D.; Howard, G. C.; Phan, J.; Acharya, P.; Macdonald, J. D.; Cheng, K.; Lorey, S. L.; Lu, B.; et al. Displacement of WDR5 from Chromatin by a WIN Site Inhibitor with Picomolar Affinity. *Cell Rep.* **2019**, *26* (11), 2916–2928.e13.
- (34) Tian, J.; Teuscher, K. B.; Aho, E. R.; Alvarado, J. R.; Mills, J. J.; Meyers, K. M.; Gogliotti, R. D.; Han, C.; Macdonald, J. D.; Sai, J.; et al. Discovery and Structure-Based Optimization of Potent and Selective WD Repeat Domain 5 (WDR5) Inhibitors Containing a Dihydroisoquinolinone Bicyclic Core. *J. Med. Chem.* **2020**, *63* (2), 656–675.
- (35) Teuscher, K. B.; Meyers, K. M.; Wei, Q.; Mills, J. J.; Tian, J.; Alvarado, J.; Sai, J.; Van Meveren, M.; South, T. M.; Rietz, T. A.; et al. Discovery of Potent Orally Bioavailable WD Repeat Domain 5 (WDR5) Inhibitors Using a Pharmacophore-Based Optimization. *J. Med. Chem.* **2022**, *65* (8), 6287–6312.
- (36) Chen, W.; Chen, X.; Li, D.; Zhou, J.; Jiang, Z.; You, Q.; Guo, X. Discovery of DDO-2213 as a Potent and Orally Bioavailable Inhibitor of the WDR5-Mixed Lineage Leukemia 1 Protein-Protein Interaction for the Treatment of MLL Fusion Leukemia. *J. Med. Chem.* **2021**, *64* (12), 8221–8245.
- (37) Teuscher, K. B.; Chowdhury, S.; Meyers, K. M.; Tian, J.; Sai, J.; Van Meveren, M.; South, T. M.; Sensintaffar, J. L.; Rietz, T. A.; Goswami, S.; et al. Structure-based discovery of potent WD repeat domain 5 inhibitors that demonstrate efficacy and safety in preclinical animal models. *Proc. Natl. Acad. Sci. U.S.A.* **2023**, *120* (1), No. e2211297120.
- (38) Macdonald, J. D.; Chacon Simon, S.; Han, C.; Wang, F.; Shaw, J. G.; Howes, J. E.; Sai, J.; Yuh, J. P.; Camper, D.; Alicie, B. M.; et al. Discovery and Optimization of Salicylic Acid-Derived Sulfonamide Inhibitors of the WD Repeat-Containing Protein 5-MYC Protein-Protein Interaction. *J. Med. Chem.* **2019**, *62* (24), 11232–11259.
- (39) Chacon Simon, S.; Wang, F.; Thomas, L. R.; Phan, J.; Zhao, B.; Olejniczak, E. T.; Macdonald, J. D.; Shaw, J. G.; Schlund, C.; Payne, W.; et al. Discovery of WD Repeat-Containing Protein 5 (WDR5)-MYC Inhibitors Using Fragment-Based Methods and Structure-Based Design. *J. Med. Chem.* **2020**, *63* (8), 4315–4333.
- (40) Ding, J.; Li, G.; Liu, H.; Liu, L.; Lin, Y.; Gao, J.; Zhou, G.; Shen, L.; Zhao, M.; Yu, Y.; et al. Discovery of Potent Small-Molecule Inhibitors of WDR5-MYC Interaction. *ACS Chem. Biol.* **2023**, *18* (1), 34–40.
- (41) Dale, B.; Cheng, M.; Park, K. S.; Kaniskan, H. U.; Xiong, Y.; Jin, J. Advancing targeted protein degradation for cancer therapy. *Nat. Rev. Cancer* **2021**, *21* (10), 638–654.
- (42) Li, K.; Crews, C. M. PROTACs: past, present and future. *Chem. Soc. Rev.* **2022**, *51* (12), 5214–5236.
- (43) Bekes, M.; Langley, D. R.; Crews, C. M. PROTAC targeted protein degraders: the past is prologue. *Nat. Rev. Drug Discovery* **2022**, *21* (3), 181–200.
- (44) He, M.; Cao, C.; Ni, Z.; Liu, Y.; Song, P.; Hao, S.; He, Y.; Sun, X.; Rao, Y. PROTACs: great opportunities for academia and industry (an update from 2020 to 2021). *Signal Transduction Targeted Ther.* **2022**, *7* (1), 181.
- (45) Kabir, M.; Yu, X.; Kaniskan, H. U.; Jin, J. Chemically induced degradation of epigenetic targets. *Chem. Soc. Rev.* **2023**, *52* (13), 4313–4342.
- (46) Gao, H.; Sun, X.; Rao, Y. PROTAC Technology: Opportunities and Challenges. *ACS Med. Chem. Lett.* **2020**, *11* (3), 237–240.
- (47) Sun, D.; Zhang, J.; Dong, G.; He, S.; Sheng, C. Blocking Non-enzymatic Functions by PROTAC-Mediated Targeted Protein Degradation. *J. Med. Chem.* **2022**, *65* (21), 14276–14288.
- (48) Yu, X.; Li, D.; Kottur, J.; Shen, Y.; Kim, H. S.; Park, K. S.; Tsai, Y. H.; Gong, W.; Wang, J.; Suzuki, K.; et al. A selective WDR5 degrader inhibits acute myeloid leukemia in patient-derived mouse models. *Sci. Transl. Med.* **2021**, *13* (613), No. eabj1578.
- (49) Dolle, A.; Adhikari, B.; Kramer, A.; Weckesser, J.; Berner, N.; Berger, L. M.; Diebold, M.; Szweczyk, M. M.; Barsyte-Lovejoy, D.; Arrowsmith, C. H.; et al. Design, Synthesis, and Evaluation of WD-Repeat-Containing Protein 5 (WDR5) Degraders. *J. Med. Chem.* **2021**, *64* (15), 10682–10710.
- (50) Li, D.; Yu, X.; Kottur, J.; Gong, W.; Zhang, Z.; Storey, A. J.; Tsai, Y. H.; Uryu, H.; Shen, Y.; Byrum, S. D.; et al. Discovery of a dual WDR5 and Ikaros PROTAC degrader as an anti-cancer therapeutic. *Oncogene* **2022**, *41* (24), 3328–3340.
- (51) Al-Awar, R. Z.-V.; Zepeda-Velazquez, C. A.; Poda, G.; Isaac, M.; Uehling, D.; Wilson, B.; Joseph, B.; Liu, Y.; Subramanlan, P.; Mamai, A.; Prakesch, M.; Stille, J. K. Inhibitors of WDR5 protein-

protein binding cross-reference to related applications. WO 2017147700 A1, 2017.

(52) Yu, X.; Xu, J.; Xie, L.; Wang, L.; Shen, Y.; Cahuzac, K. M.; Chen, X.; Liu, J.; Parsons, R. E.; Jin, J. Design, Synthesis, and Evaluation of Potent, Selective, and Bioavailable AKT Kinase Degraders. *J. Med. Chem.* **2021**, *64* (24), 18054–18081.

(53) Yu, X.; Xu, J.; Cahuzac, K. M.; Xie, L.; Shen, Y.; Chen, X.; Liu, J.; Parsons, R. E.; Jin, J. Novel Allosteric Inhibitor-Derived AKT Proteolysis Targeting Chimeras (PROTACs) Enable Potent and Selective AKT Degradation in KRAS/BRAF Mutant Cells. *J. Med. Chem.* **2022**, *65* (20), 14237–14260.

(54) Jiang, B.; Wang, E. S.; Donovan, K. A.; Liang, Y.; Fischer, E. S.; Zhang, T.; Gray, N. S. Development of Dual and Selective Degraders of Cyclin-Dependent Kinases 4 and 6. *Angew. Chem., Int. Ed. Engl.* **2019**, *58* (19), 6321–6326.

(55) Yu, X.; Xu, J.; Shen, Y.; Cahuzac, K. M.; Park, K. S.; Dale, B.; Liu, J.; Parsons, R. E.; Jin, J. Discovery of Potent, Selective, and In Vivo Efficacious AKT Kinase Protein Degraders via Structure-Activity Relationship Studies. *J. Med. Chem.* **2022**, *65* (4), 3644–3666.

(56) Meng, F.; Xu, C.; Park, K. S.; Kaniskan, H. U.; Wang, G. G.; Jin, J. Discovery of a First-in-Class Degradator for Nuclear Receptor Binding SET Domain Protein 2 (NSD2) and Ikaros/Aiolos. *J. Med. Chem.* **2022**, *65* (15), 10611–10625.

(57) Cheng, M.; Yu, X.; Lu, K.; Xie, L.; Wang, L.; Meng, F.; Han, X.; Chen, X.; Liu, J.; Xiong, Y.; et al. Discovery of Potent and Selective Epidermal Growth Factor Receptor (EGFR) Bifunctional Small-Molecule Degraders. *J. Med. Chem.* **2020**, *63* (3), 1216–1232.

(58) Yu, X.; Cheng, M.; Lu, K.; Shen, Y.; Zhong, Y.; Liu, J.; Xiong, Y.; Jin, J. Exploring Degradation of Mutant and Wild-Type Epidermal Growth Factor Receptors Induced by Proteolysis-Targeting Chimeras. *J. Med. Chem.* **2022**, *65* (12), 8416–8443.

(59) Cai, L.; Rothbart, S. B.; Lu, R.; Xu, B.; Chen, W. Y.; Tripathy, A.; Rockowitz, S.; Zheng, D.; Patel, D. J.; Allis, C. D.; et al. An H3K36 methylation-engaging Tudor motif of polycomb-like proteins mediates PRC2 complex targeting. *Mol. Cell* **2013**, *49* (3), 571–582.